Atmospheric ^{10}Be from Talos Dome (East Antarctic) ice core records geomagnetic dipole intensity from 170 to 270 ka BP

Alexis Lamothe[1], Edouard Bard[1], Nicolas Thouveny[1], Ellyn Auriol[1], Mirko Severi[2], Rita Traversi[2], Martine De Angelis[3], Frank Wilhelms[4,5], Robert Mulvaney[6], Fawzi Zaidi[1], Georges Aumaitre[1], Karim Keddadouche[1], Mélanie Baroni[1]

[1]Aix Marseille Univ, CNRS, IRD, INRAE, Coll France, CEREGE, Aix-en-Provence, France
[2]Department of Chemistry "Ugo Schiff", University of Florence, Florence, Italy
[3]Univ. Grenoble Alpes, CNRS, IRD, INRAE, Grenoble INP, IGE, 38000 Grenoble, France
[4]Alfred-Wegener-Institut Helmholtz-Zentrum für Polar-und Meeresforschung, Bremerhaven, Germany
[5]Georg-August-Universität, Geowissenschaftliches Zentrum, Abteilung Isotopengeologie, Goldschmidtstraße 1, D-37073 Göttingen
[6]British Antarctic Survey, Cambridge, UK
Correspondence to: Alexis Lamothe (lamothe@cerege.fr)

Abstract. We present high-resolution ^{10}Be concentration and flux records from the Talos Dome ice core (East Antarctica), covering the period from 170 to 270 ka BP, to assess the capacity of Antarctic ice cores to capture the dipole moment reductions triggered by geomagnetic excursions of different amplitudes. Three distinct geomagnetic events are identified in the ^{10}Be flux. The dipole collapse linked to the Iceland Basin Excursion (IBE) is clearly recorded as a ^{10}Be peak flux 1.59 to 2.08 times above background between (192.0 ± 1.4) ka BP and (185.6 ± 1.4) ka BP. A clear asymmetric structure is observed, with a rapid decline of the geomagnetic dipole, followed by a three-step recovery. Two dipole decreases of lower amplitude are also resolved in relation with the Pringle Falls Excursion (PFE), lasting from (218.5 ± 1.90) to (206.0 ± 0.8) ka BP, and the Mamaku Excursion (ME), identified at (242.0 ± 0.3) ka BP, both showing an increase of the ^{10}Be flux by a factor of 1.24 to 1.63. A total of 52 short-term ^{10}Be concentration minima were also identified and are consistently associated with peaks in major ion concentrations, indicating post-depositional effects that affect concentration but not the longer-term flux signal. Comparison with Dome Fuji ice core and oceanic authigenic ^{10}Be/^{9}Be records reveals strong agreement in the timing and structure of the dipole moment collapses linked with these excursions. These results further support the use of ^{10}Be for synchronizing ice and marine archives as well as to reconstruct past geomagnetic dipole moment variations and refining age models over the Pleistocene.

1 Introduction

The intensity of the geomagnetic dipole has varied over geological timescales (e.g., Bono et al., 2022). Among these variations, full geomagnetic reversals as well as incomplete or short-lived reversals, commonly referred to as excursions, are of particular interest for studying the dynamics of the geomagnetic dipole moment (GDM). Recent models suggest that the GDM fluctuations can be explained by stochastic variations in heat transfer between the Earth's core and mantle (e.g. Molina-Cardín

et al., 2021). However, the geodynamo may also exhibit deterministic but chaotic behaviour (Gissinger, 2012; Müller et al., 2025; Ryan and Sarson, 2007) – that is, governed by nonlinear physical laws but highly sensitive to initial conditions. Recurrent features observed in paleomagnetic records support this view, implying that the apparent stochasticity of GDM variations may partly emerge from underlying deterministic dynamics. Nevertheless, this stochastic assumption remains a pragmatic first-order approximation due to the complexity of modelling the geodynamo and the sparse, indirect, and high uncertainties in observational data. Ultimately, progress in understanding the chaotic behaviour of the geodynamo hinges on the availability of reliable, high-resolution, synchronous, and cross-validated records of GDM variations, as this study aims to report between 170 ka BP and 270 ka BP.

Paleomagnetic excursions are the most common manifestations of these large amplitude variations of the GDM. Unlike secular variations – for which the virtual geomagnetic pole (VGP) motion within a cone of 45° around the geographic pole – paleomagnetic excursions consist in large amplitude, though transient, departures of the virtual geomagnetic pole beyond 45° away from the Earth rotation axis. Such events have been reconstructed from paleomagnetic studies of various geological archives such as volcanic sequences (e.g., Champion et al., 1988), marine (e.g., Valet and Meynadier, 1993) and lacustrine sediments (e.g., Oda et al., 2002). In both excursions and full reversals, the dipole moment decreases prior to the VGP migration, while the recovery of field intensity occurs after the return to a stable polarity state, either in the original or in the reversed polarity (Laj et al., 2006; Valet et al., 2005). When recorded from various and distant sites for the same event, these large amplitude intensity variations express the decrease and the subsequent recovery of the GDM, concomitant with the VGP migration.

The Iceland Basin Excursion (IBE, naming and dating of the event is discussed in section 2.1), dated to approximately 190 ka BP, is probably the strongest excursion during the Bruhnes chron (< 780 ka BP) based on GDM intensity reconstruction (Simon et al., 2016) and has been recorded in the Icelandic basin sediment as a full but transient reversal (Channell et al., 1997). Dipole intensity reduction has been estimated between 70 % (Yamamoto et al., 2010) and 80 % (Simon et al., 2020) relative to the pre-event background dipole moment. Such a significant collapse indeed reaches the threshold of full reversal (Valet et al., 2008), making the IBE ideal to understand GDM variations. Additionally, the intensity and global detectability of IBE make it optimal for archive synchronisation (e.g., Leduc et al., 2006), particularly between sediment and ice core records, where the phase relationship appears minimal (Horiuchi et al., 2016; Simon et al., 2016).

Cosmogenic radionuclides, such as beryllium-10 (^{10}Be), offer a valuable proxy for reconstructing geomagnetic intensity changes. Atmospheric ^{10}Be mainly results from spallation reactions between galactic cosmic rays and atmospheric oxygen and nitrogen atoms (e.g., Poluianov et al., 2016). Between 60 and 66 % of its atmospheric production occurs in the stratosphere (Golubenko et al., 2022; Poluianov et al., 2016; Zheng et al., 2024). As the flux of highly energetic particles is modulated by GDM strength, ^{10}Be atmospheric production, and subsequent deposition into archives, is correlated with the Virtual Axial Dipole Moment (VADM) intensity (Carcaillet et al., 2004; Simon et al., 2016). The concentration of ^{10}Be in paleoarchives can thus provide records of the dipole moment variations that can be compared with relative paleointensity ones. While sediment records provide long temporal coverage spanning several Ma (Valet et al., 2025), they may be affected by oceanic circulation

(Savranskaia et al., 2024) and sedimentary remobilization (Savranskaia et al., 2021), complicating ^{10}Be-based interpretations. In contrast, ice core ^{10}Be records offer more direct and temporally resolved signals, though they may be altered by snow accumulation variability (e.g., Yiou et al., 1985) and post-depositional processes (e.g., Kappelt et al., 2025; Raisbeck et al., 2006).

As efforts intensify to develop robust dating tools for oldest Antarctic ice (Wolff et al., 2022), potentially extending beyond 1.5 Ma (Chung et al., 2025), cosmogenic nuclide records have gained prominence not only for reconstructing GDM variations, but also for enabling stratigraphic correlations between sediment and ice core archives. To date, few studies have explored geomagnetic excursions in ice cores, and those that do typically focus on high-amplitude events such as the Laschamps, ≈41 ka BP (Raisbeck et al., 2017) and the IBE (Horiuchi et al., 2016). Here, we investigate the capacity of ice cores to capture both high- and low-amplitude excursions, respectively the IBE and the two Pringle Falls excursions also named Mamaku or Jamaica (see section 2 for a literature review on the naming of the events), by presenting the longest ^{10}Be record from an ice core currently available. Our ^{10}Be record from Talos Dome (East Antarctica) is compared with the IBE record from Dome Fuji (Horiuchi et al., 2016), as well as with sedimentary records based on authigenic ^{10}Be/^{9}Be (Frank et al., 1997; Horiuchi et al., 2016; Simon et al., 2016). In this context, we assess the fidelity of ice core ^{10}Be as a reliable paleomagnetic proxy and synchronise ocean and ice archives over the 170 ka BP – 270 ka BP interval.

2 Excursions between 170 and 250 ka BP: a review

Between 170 ka BP and 250 ka BP, several geomagnetic excursions have been reported (Figure 1) with different names, sometimes referring to the same event. In order to help the reader understanding this confusing literature, we provide a short overview.

2.1 The 190 ka BP excursion

The geomagnetic excursion dated to ≈190 ka BP, now widely referred to as the Iceland Basin Excursion (IBE), is considered one of the most significant geomagnetic events of the Brunhes Chron (Simon et al., 2016). One of the first attempts to date this excursion with high confidence came from lava flows, notably in the Snake River Plain (Idaho, USA). Champion et al. (1981, 1988) reported transitional paleomagnetic directions in multiple flow units, including Site E in Idaho, and proposed a Potassium-Argon (K-Ar) age of (188 ± 8) ka BP. They named this event the Jamaica excursion, based on terminology used in earlier literature (Ryan, 1972). This naming particularly persisted in the literature related to volcanology.

Subsequent studies began identifying concomitant excursions in marine sediment cores, particularly in the Pacific. Tauxe & Wu (1990) reported excursion-like signals from two cores on the Ontong Java Plateau (ERDC-89P and ERDC-113P), with age estimates around 190 ka BP. Around the same time, Valet and Meynadier (1993) published data from ODP Sites 848 and 851 showing an excursion between 180 and 200 ka BP, which they tentatively linked to the Jamaica event described by Champion et al. (1981, 1988). Records from the western equatorial Pacific also reported an excursion around that age identified

in cores NP5, NP7, NGC16, and NGC29 (Yamazaki and Ioka, 1994), later extended to NP35, NGC36, and NGC38 (Yamazaki et al., 1995).

Highly-resolved analyses of North Atlantic sediment cores confirmed the existence of a short, high-amplitude, and global excursion around 190 ka BP (Weeks et al., 1995), that was associated to the Jamaica event, referring to Champion et al., (1988). Other sites further supported these conclusions including a suite of eight cores from the Indian and Western Pacific Oceans (Guyodo and Valet, 1996), three cores from the Acores regions (Lehman et al., 1996), and from Northwest Pacific (Roberts et al., 1997). The name Iceland Basin Excursion was formally introduced in 1997 based on high-resolution magnetic studies of sediment core collected from the Iceland Basin, ODP sites 983 and 984 (Channell, 1999; Channell et al., 1997). Both sites of the Iceland Basin revealed a short full reversal event at ≈186–189 ka BP with magnetization components rotating through 180° and back, in coincidence with a relative paleointensity (RPI) low of approximately 3 ka. These records as well as the other studies from that region (listed below), led to widespread adoption of the term Iceland Basin Excursion.

Since 1997, numerous studies have reported the IBE across a wide range of archives and locations. Here, we provide a non-exhaustive list of these observations. IBE has been robustly documented at multiple ODP sites along the Western and Eastern North Atlantic: Sites 1061, 1062, and 1063 (Channell et al., 2012; Christl et al., 2010; Knudsen et al., 2008; Laj et al., 2006; ODP Leg 172 Scientific Party et al., 1998, p.172), as well as at Sites 980, 984, and 919 (Channell, 2006, 1999; Channell and Raymo, 2003). Additional detections were reported from the Labrador basin (Stoner et al., 1998), Western and Equatorial Pacific cores (Gee et al., 2000), Lake Baikal (Demory et al., 2005; Oda et al., 2002), Southern Ocean (Stoner et al., 2003), the Portuguese margin (Thouveny et al., 2004), and the Irminger Basin and the Eirik Drift (Evans et al., 2007). IBE was first observed with authigenic ^{10}Be measurements from Portuguese margin marine cores MD95-2040 and MD95-2042 (Carcaillet et al., 2004; Knudsen et al., 2008). IBE was reported in a lava flow at Unzen Volcano (Japan) with a K-Ar age of (197 ±17) ka BP (Shibuya et al., 2007). Further establishing its global extent, the GDM low linked to IBE has also been observed in an Antarctic ice core with atmospheric ^{10}Be concentrations from Dome Fuji (Horiuchi et al., 2016). Because of its global characteristics, global stack compilations are representative of the collapse of GDM during IBE (Channell, 2014; Simon et al., 2016; Valet et al., 2020, 2024).

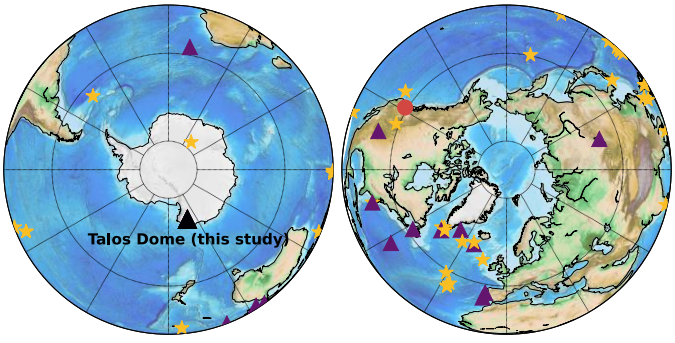

Figure 1: *Map of sites found in literature recording at least one of the geomagnetic excursions discussed in this paper: the three excursions (IBE, PFE and ME, triangles), IBE alone (stars), or PFE alone (circle). The references are listed in Table S1.*

2.2 Excursion(s?) between 205 and 245 ka BP

Several geomagnetic excursions have been identified in the 205–245 ka BP interval, but their amplitude, naming end even number remain debated. Herrero-Bervera et al. (1994) provided one of the most comprehensive syntheses of an RPI low dated to (218 ± 10) ka BP with $^{40}Ar/^{39}Ar$ across multiple western U.S. sites: Pringle Falls – which gave its name to the event – and Summer Lake (Oregon), Mono Lake (Paoha Island), and Benton Crossing (Long Valley, California), although the first observation of a geomagnetic event around that age was probably observed in lava flows from Albuquerque (Geissman et al., 1990). Given dating uncertainties, some studies associated the Pringle Falls excursion to the Jamaica excursion (Langereis et al., 1997). In the Southern hemisphere, a prominent geomagnetic reversal was recorded in the Mamaku ignimbrite, erupted from the Taupo volcanic zone, New Zealand. This event has been dated using $^{40}Ar/^{39}Ar$ methods at (227 ± 8) ka BP (Houghton et al., 1995; Tanaka et al., 1996), with revised estimates at (223 ± 3) ka BP based on improved chronostratigraphy (Mcwilliams, 2001). Updated dating of the excursion recorded in Albuquerque lavas and Pringle Falls ash D – (218 ± 14) ka BP and (211 ± 13) ka BP, respectively – supported that all three sites (Albuquerque, Pringle Falls, Mamaku) likely recorded the same geomagnetic excursion, named Pringle Falls, and dated to (211 ± 13) ka BP (Singer et al., 2008).

However, sediment records complicated this interpretation. For instance, RPI minima were observed around 208 ka BP (Channell, 2006) and 238 ka BP (Channell et al., 2012) in Atlantic sediment cores. Besides, a long minimum is observed in the PISO-1500 stack between 208 and 221 ka BP, while a sharp, decoupled minimum is recorded around 238 ka BP (Channell et al., 2009). This led to question the existence of two, instead of a unique, 'Pringle Falls' excursions.

In this sense, the comparison of RPI and cosmogenic nuclide concentrations would solve this ambiguity. Between 210 and 220 ka BP, the RPI low correlates with a cosmogenic nuclide production enhancement, while a marked RPI low and a minor cosmogenic nuclide production enhancement occurs at ca. 236 ka BP (Simon et al., 2016). However, the latter has also been dated around (230 ± 12) ka BP in Mamaku lavas (Shane et al., 1994). Finally, a small amplitude RPI low has been observed around 250–255 ka BP concomitant with a clear enhancement in authigenic $^{10}Be/^{9}Be$ measured in two West Equatorial Pacific Ocean sediment cores (Simon et al., 2016). This event could correspond to the Calabrian Ridge 0 excursion (Mediterranean Sea, Langereis et al., 1997), the 8α excursion (IODP Leg 172 Sites 1060–1063, Lund et al., 2001), and the Fram strait excursion (Nowaczyk and Frederichs, 1999).

Consequently, a continuous, globally-representative and well-dated record like ice core ^{10}Be from Antarctica would provide valuable information to better understand low-amplitude excursions. However, until now, no study has discussed this double excursion. This literature synthesis supports a cautious approach for dating and identifying the Pringle Falls, Mamaku and Calabrian Ridge 0-like excursion(s?).

To give credit to all these previous studies we will give consensual names to the three excursions we study in this work: the Iceland Basin Excursion (IBE), the Pringle Falls-Excursion (PFE), and the Mamaku Excursion (ME), dated around 190 ka BP, 210 ka BP, and 240 ka BP, respectively.

3 Material, methods, and chronology

3.1 Talos Dome ice core

Measurements of ^{10}Be have been performed in the Talos Dome ice core (TALDICE). Talos Dome is situated on the East Antarctic plateau (72°48'S, 159°06'E; 2316 m a.s.l., Figure 1), being particularly close to oceans (290 km from the Southern Ocean and 250 km from the Ross Sea) than other drillings like EPICA Dome C (EDC) or Dome Fuji (DF) (Frezzotti et al., 2004). The drilling campaign reached 1,620 m, being 175 m above the bedrock (Crotti et al., 2021). It is worthnoting that the drilling was situated in a glacial valley, whose hills reach 1,550 m (Crotti et al., 2021).

The ice core was continuously sampled in sections of 20 cm (when possible) between 1470 m and 1499 m and between 1505 m and 1531 m, with a non-sampled section between 1499 and 1505 m. The outermost section of the ice core, dedicated to cosmogenic nuclide measurements, had been stored in clean polyethylene bags at -20°C in a cooling facility, close to CEREGE. As part of the LGO2i platform at CEREGE research institute, the ice samples were cut with a saw pre-decontaminated with ultrapure ice and the outermost 1 mm of ice was removed with a ceramic knife. Ice samples were always handled with clean nitrile gloves, and left to melt in glass beakers, covered with plastic film, at room temperature.

In order to compare with ^{10}Be fluxes from Dome C over the last century, 11 samples have been measured from TALDICE firn between 4.5 m and 10 m with a resolution of 50 cm.

3.2 Concentration measurements

3.2.1 Concentrations of ^{10}Be

Concentrations of ^{10}Be were obtained following the protocol developed in Raisbeck et al., (2006) and Baroni et al., (2011) and measurements were made on the French Accelerator Mass Spectrometer (AMS) national facility, ASTER (Arnold et al., 2010) as part of the LN2C analytical platform.

On average, 257 samples of approximately 20 cm corresponded to a mean mass of (121 ± 10) g (± 1σ). A ^{9}Be carrier solution (10^{-3} g g^{-1} ™Scharlau) was added to each sample with a mean added mass of (0.253 ± 0.001) g, in order to set the ^{10}Be/^{9}Be ratio prior to any chemical reaction. Preconcentration and purification of Be samples was performed with cation exchange resins (Dionex AG 50W-X8) and eluted with 12 mL of HNO_3 (3M). Beryllium dihydroxide was subsequently formed adding 1.7 mL of NH_3 (28 %). The precipitate was rinsed twice with 15 mL of a NH_3/H_2O solution (500 mL H_2O/120µL of NH_3 (28%)) prior to be dissolved with 250 µL of HNO_3 (69 %). The beryllium nitrate solution was evaporated at 240°C in a crucible. After the final pyrolysis step held at 900°C, the beryllium oxide powder was mixed with niobium powder (in approximately the same mass), and subsequently pressed into a copper cathode. The samples were subsequently measured on

the ASTER AMS (Arnold et al., 2010). The $^{10}Be/^{9}Be$ ratio is normalized to the in-house standard that has a $^{10}Be/^{9}Be$ ratio of $(1.191 \pm 0.013) \times 10^{-11}$ at at^{-1} (Braucher et al., 2015) for a ^{10}Be half-life of (1.387 ± 0.012) Ma (Chmeleff et al., 2010; Korschinek et al., 2010).

In addition to the 257 samples, 13 blanks had been measured, made from 100 mL of ultra-pure water (18.2 MΩ cm), with a mean $^{10}Be/^{9}Be$ ratios of $(4.2 \pm 0.3) \times 10^{-15}$ at at^{-1}. In comparison, the $^{10}Be/^{9}Be$ sample ratio mean value is $(8.3 \pm 3.4) \times 10^{-14}$ at at^{-1}. Propagating the counting statistics and all uncertainties related to the chemical preparation and the sample measurements yielded a mean 2σ uncertainty of 6.8 % for the samples. Consequently, the mean ^{10}Be concentration was $(2.51 \pm 0.08) \times 10^{4}$ at g^{-1}.

3.2.2 Major ions

The concentrations of the major ions were measured by classical ion chromatography methods on discrete samples (Morganti et al., 2007). These samples were collected into sample vials using a melting device (Severi et al., 2015) connected to a fraction collector in the cold laboratory of the Alfred Wegner Institute in Bremerhaven. The melter was specifically designed in order to sample just the uncontaminated inner part of each ice core section discarding the possibly contaminated outer layers. The discrete samples were then distributed for analysis among four different laboratories for analysis: University of Florence (Italy), BAS (Cambridge, United-Kingdom), IGE (ex-LGGE, Grenoble, France), and AWI (Bremerhaven, Germany). No inter-laboratory comparison was performed, and each laboratory analyzed a distinct subset of samples. However, all laboratories followed the same ion chromatography analytical protocols and procedures as those applied to the EPICA Dome C and EPICA Dronning Maud Land ice cores, for which inter-laboratory comparisons demonstrated very good agreement (Littot et al., 2002). Systematic inter-laboratory differences are therefore expected to be negligible for the TALDICE dataset.The ions measured by each laboratory on the discrete samples were 5 anions (Cl^-, $CH_3SO_3^-$ (methane sulfonic acid, MSA), F^-, NO_3^-, and SO_4^{2-}) and 5 cations (Na^+, NH_4^+, K^+, Mg^{2+}, and Ca^{2+}). Measurements were made with a mean resolution of 8 cm (maximum 17 cm). Details about blanks and calibrations are reported in Morganti et al. (2007).

The final dataset, obtained by merging the data from the four laboratories, was finally reprocessed by hand, removing outliers resulting from probable contamination events. Specifically, outliers were removed when values were affected by probable contamination events or analytical artifacts, such as isolated spikes inconsistent with adjacent samples. In the end, between 1470 and 1531 m, post-processing resulted in the withdrawal of 0 %, 19 %, 3 %, 0 %, 0 %, 2 %, 1 %, 0 %, 0 %, and 0 % of the total sample depths for Na^+, NH_4^+, K^+, Mg^{2+}, Ca^{2+}, Cl^-, MSA, F^-, NO_3^-, and SO_4^{2-}, respectively. The acidity profile was reconstructed following an ionic balance ($[H^+] = [NO_3^-] + [SO_4^{2-}] + [Cl^-] + [MSA] + [F^-] - [Ca^{2+}] - [Mg^{2+}] - [K^+] - [Na^+] - [NH_4^+]$ in $\mu Eq\ L^{-1}$).

3.3 AICC2023 chronology and ^{10}Be flux

The AICC2023 chronology (Bouchet et al., 2023) was used to date the ice, spanning from (172.3 ± 1.9) ka BP to (275.7 ± 1.8) ka BP. Our record covers several transitions from glacial to interglacial periods, from Marine Isotope Stage (MIS) 6.4 to 8.3

(Railsback et al., 2015). Therefore, the annual snow accumulation rate, provided by the AICC2023 chronology, ranges between (4.3 ± 0.8) cm a^{-1} and (8.1 ± 1.5) cm a^{-1} with a mean value of 5.5 cm a^{-1}. On average, the ≈20 cm resolution corresponds to ≈300 years (min = 60 a; max = 1,375 a).

The flux of ^{10}Be was calculated as ^{10}Be concentration × snow accumulation rate × ice density (i.e., 0.917 g cm^{-3}). A half-life corrected flux was also calculated, using the (1.387 ± 0.012) Ma ^{10}Be half-life (Chmeleff et al., 2010; Korschinek et al., 2010). The resulting mean half-life-corrected ^{10}Be flux is (1.36 ± 0.26) × 10^5 at cm^{-2} a^{-1}, considering uncertainty on ^{10}Be concentration, snow accumulation rate, and ^{10}Be half-life. Although this calculation is numerically valid, it likely overestimates the uncertainty associated with accumulation rate. Indeed, in the AICC2023 chronology, uncertainties on snow accumulation rate are inherited from the Paleochrono Bayesian framework (Parrenin et al., 2024) and strongly depend on the input uncertainties. During the interval 170–270 ka BP, the relative age uncertainty is only ±1 %, whereas the relative uncertainty in accumulation rates reaches ±20 % (Bouchet et al., 2023). This large value reflects the prior uncertainty (20 %) assigned to accumulation scenarios, which are derived from a poorly constrained empirical relationship between present-day water isotope in the snow and accumulation (Parrenin et al., 2007). In Paleochrono, such prior scenarios are iteratively adjusted within their uncertainty range to fit the dated horizons. In the AICC2023 simulation, posterior age estimates are constrained, but accumulation variations remain loosely constrained. Consequently, the ±20 % snow accumulation rate uncertainty that would arise from directly propagating the AICC2023 accumulation error is likely overestimated and further work is needed to estimate precisely the uncertainty in accumulation scenarios (Bouchet, personal communication).

In order to avoid artificial inflation of the uncertainty associated with ^{10}Be flux variations, we propose a more realistic uncertainty propagation to track relative changes through time rather than absolute flux values. Rather than propagating the full absolute uncertainty of the snow accumulation rate, we use the 20 % accumulation rate uncertainty from AICC2023 as a relative uncertainty (0.2) applied to deviations from the mean accumulation rate (Equation 1). With this formulation, accumulation rates equal to the mean have no associated uncertainty in terms of variability, although they remain subject to absolute uncertainty. This approach therefore does not represent the total uncertainty of the accumulation rate, but rather a 'variation uncertainty' that reflects how uncertainty in accumulation affects the amplitude of ^{10}Be flux fluctuations. This corrected uncertainty reflects the fact that variability in ^{10}Be flux is primarily driven by changes in accumulation over time rather than by its absolute range of uncertainty. On average, the corrected uncertainty, used when interpreting ^{10}Be flux variations as in Figure 1, is 22 % (min 0.2 %; max 53 %) lower than the raw uncertainty.

$$Corrected\_uncertainty(t)\ (/\%) = \frac{|accumulation(t) - accumulation_{mean\ (170-270\ ka)}| \times 0.2}{accumulation(t)} \qquad \text{Equation 1}$$

Prior to comparison with the TALDICE record, the Dome Fuji ^{10}Be fluxes (Horiuchi et al., 2016) were recalculated using the more recent accumulation rate. The DF record spans a period from 170 ka BP to 205 ka BP. While the record was published using the DFO-2006 chronology (Kawamura et al., 2007) with snow accumulation rate being retrieved from Parrenin et al., (2007), ^{10}Be fluxes were corrected using the most recent DF chronology, DF2021 (Oyabu et al., 2022).

To identify anomalously low ^{10}Be fluxes, which could bias the interpretation of geomagnetic intensity, we applied an objective statistical criterion. These ^{10}Be minima were identified when the concentration fell below the mean minus one standard deviation, both calculated using a 3-ka rolling window. The outlier analysis was intentionally focused on minima, as low ^{10}Be values are far more frequent and have a strong impact on the rolling average than high values.

4 Results

4.1. ^{10}Be concentration and flux

Between 170 ka BP and 270 ka BP, TALDICE ^{10}Be concentrations vary between $(0.25 \pm 0.03) \times 10^4$ at g^{-1} and $(7.1 \pm 0.2) \times 10^4$ at g^{-1}, with mean concentration and uncertainty values of 2.5×10^4 at g^{-1} and 0.08×10^4 at g^{-1}, respectively (Figure 2A). This period spans MIS 8 to 6, including Termination III and the MIS 7, a time marked by pronounced climatic fluctuations (Railsback et al., 2015) (Figure 2C). After accounting for variations in snow accumulation rates using the AICC2023 chronology (Bouchet et al., 2023), ^{10}Be fluxes show values between $(1.9 \pm 0.4) \times 10^4$ at cm^{-2} a^{-1} and $(31.0 \pm 6.1) \times 10^4$ at cm^{-2} a^{-1} (Figure 2B). These flux variations highlight notable production changes independent of deposition variations. Concurrently, VADM values fluctuated indicating intervals of geomagnetic instability (Channell et al., 2009; Simon et al., 2016). In particular, 4 geomagnetic excursions are reported with little to strong depletions of the VADM, around 190 ka BP, 215 ka BP, 240 ka BP, and 258 ka BP (Figure 2E). An increase in the ^{10}Be flux related to a background production is expected during such minima due to reduced geomagnetic shielding, discussed in Section 5.2 and 5.3. One geomagnetic excursion is already clearly recorded in TALDICE: a pronounced ^{10}Be flux peak associated with the IBE excursion around 190 ka BP. Another event, previously identified in two sediment cores from the South-West Pacific (Simon et al., 2016), likely occurred around 258 ka BP but is not recorded in TALDICE due to the absence of measurements caused by a missing section of the ice core.

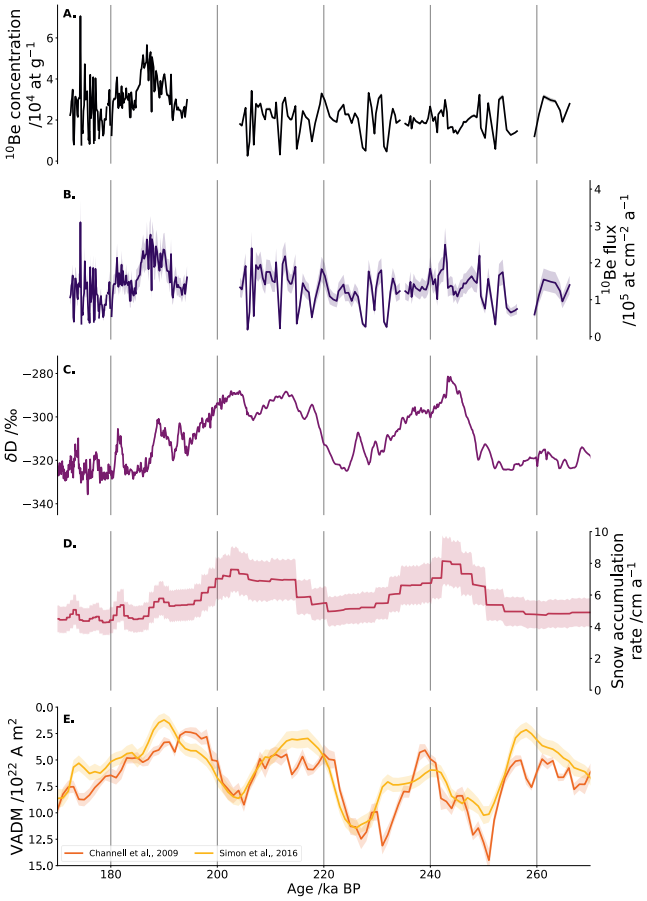

Figure 2: *A) TALDICE ^{10}Be concentration (10^4 at g^{-1}) with the concentration uncertainty (shaded black; 3.6 % on average). B) ^{10}Be flux (10^5 at cm^{-2} a^{-1}) with the uncertainty (shaded purple) which accounts for the concentration uncertainty and the variation of the accumulation (see section 4). C) Climate variations are recorded in TALDICE with δD water isotopes (‰; Stenni et al., 2011), from which Marine isotope stage can be listed (6.4 to 8.3; Railsback et al., 2015). D) Snow accumulation rate (cm a^{-1}) is retrieved from the AICC2023 chronology (Bouchet et al., 2023). E) Virtual Axial Dipole Moment (VADM, A m^2) is estimated from Relative Paleointensity (PISO-1500; Channell et al., 2009) (orange) or from authigenic ^{10}Be/^{9}Be (Simon et al., 2016). Note that the y-axis is reversed.*

4.2. ^{10}Be minima

A total of 40 minima in ^{10}Be concentration were identified across the TALDICE record studied in this work, which appear to coincide with maxima in the concentrations of major ions (Figure 3). This association is statistically significant (permutation test's *p*-value = 0.0001), though no direct quantitative relationship can be established. The major ions involved originate from a variety of sources, including oceanic sea spray (Na^+, Cl^-, Mg^{2+}, MSA, SO_4^{2-}), crustal dust (Ca^{2+}, Mg^{2+}), and volcanic (SO_4^{2-}) sources. In addition to ion concentration peaks, many of the ^{10}Be minima are also associated with decreases in the Cl^-/Na^+

ratio which is typically used to study changes in the relative contributions of marine aerosols or alterations in transport processes (Legrand et al., 2017).

To test whether the identified ^{10}Be concentration minima preferentially occur under particular conditions, we compared their distribution against δD and [Ca^{2+}]. Of the 40 minima identified, 31 occurred during glacial intervals (δD < -300 ‰), which is proportional to the fraction of the record spent in glacial conditions (77 %). A χ^2 test confirms no significant increase in the number of minima during glacials (p = 1.00), and δD values at ^{10}Be minima are statistically indistinguishable from non-minima levels (Mann-Whitney U test, p = 0.889). In contrast, [Ca^{2+}] concentrations are systematically higher at ^{10}Be minima. While median [Ca^{2+}] is only slightly elevated at minima compared to the background (Mann–Whitney U p = 0.53), contingency tests using thresholds show strong enrichment: for example, 32 % of ^{10}Be minima exceed 15 ppb Ca^{2+} compared to 13 % of the background (χ^2 = 8.0, p = 0.005), and 7 ^{10}Be minima exceed 30 ppb compared to only 9 out of 221 non-minima samples (χ^2 = 8.4, p = 0.005). This suggests that short-lived ^{10}Be minima preferentially coincide with dust-rich conditions.

4.3. ^{10}Be background flux

After removing the 40 identified ^{10}Be minima, rolling mean averages can be calculated to smooth the record and obtain the first-order variations, which are likely to result. Testing 1 ka, 3ka and 5 ka rolling mean averages (Figure S1) illustrate the trade-off between noise reduction and signal preservation. Given the mean resolution of our record (300 a) we selected a 3-ka rolling mean average as a practical compromise. This choice provides stable background trends while preserving the amplitude of GDM-related variations. The resulting 3-ka averaged ^{10}Be flux record can be compared to geomagnetic reconstructions, including the Dome Fuji ice core data (Horiuchi et al., 2016) in Figure 4,, and authigenic ^{10}Be/^{9}Be records from marine sediment cores (Simon et al., 2016) and the ^{10}Be production (Poluianov et al., 2016) calculated from RPI-based VADM (Channell et al., 2009) in Figure 5. Flux enhancement during geomagnetic excursions or events depends strongly on the choice of background taken as reference. Here, we consider either the full 170–270 ka BP interval ^{10}Be flux mean average of (1.36 ± 0.26) × 10^5 at cm^{-2} a^{-1} or a fixed baseline of 1.1 × 10^5 at cm^{-2} a^{-1} as reference values. The latter could be considered as representative of the long-term background ^{10}Be flux, which is close to the minimum values the 3 ka rolling mean average around 178 ka BP and 223 ka BP. Depending on the chosen baseline, the flux enhancement factors during specific events are as follows: for the 190 ka BP event (IBE), the ^{10}Be flux is 1.59 or 2.08 times the background; for the 205–215 ka BP event (PFE), the increase is 1.24 or 1.62 on average; and for the 240 ka BP event (ME), the peak flux reaches 1.25 or 1.63 times the reference value. As a general idea, the flux enhancement factor for IBE represents 1.5 times the modern value of c. 1.64 10^5 at cm^{-2} a^{-1} at Dome C (Jouzel et al., 2026).

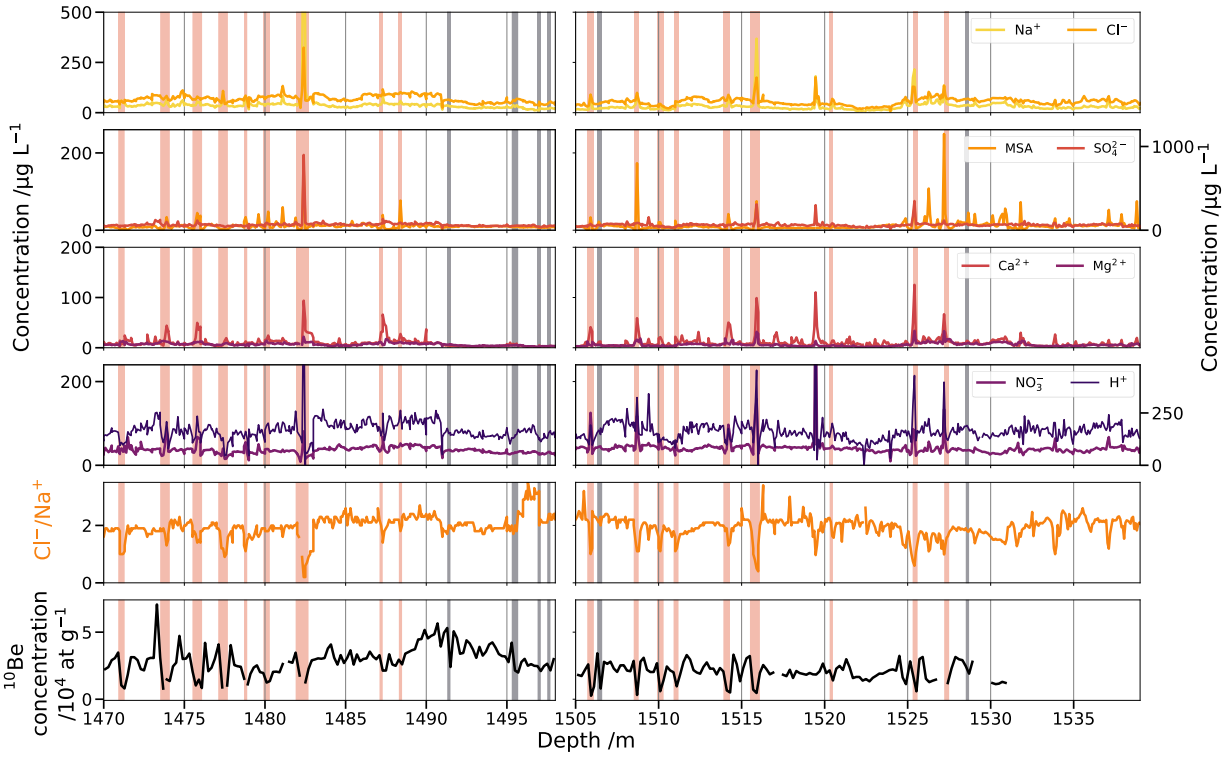

***Figure 3**: Minima in ^{10}Be concentration (black line) identified at the measurement resolution (≈20 cm) are highlighted by shaded areas. Orange shading indicates ^{10}Be minima that are concomitant with maxima in major ion concentrations, whereas grey shading indicates minima without concomitant major ion maxima. The resolutions are the measurement resolution, i.e., ≈20 cm for ^{10}Be. Because minima are defined at the ^{10}Be sampling resolution, a low-concentration interval extending over 40 cm is counted as two distinct minima. Only the 40 minima identified within the 1470–1531 m depth interval (corresponding to 170–270 ka BP) and retained for the present analysis are shown. The major ion (Na^+, Cl^-, MSA, SO_4^{2-}, Ca^{2+}, Mg^{2+}, NO_3^-, and H^+) concentration profiles are in high resolution (8 cm). Acidity profile (H^+) is calculated from an ionic balance (see section 3.2.2).*

5 Discussion

5.1 ^{10}Be abrupt minima

Post-depositional artifacts in the geomagnetically-induced ^{10}Be signal in ice cores have been widely discussed, particularly in Greenland, where dust contributions have been shown to significantly affect the total ^{10}Be budget especially during glacial periods during which the dust level are higher than during interglacials (Baumgartner et al., 1997). Among known confounding factors, snow accumulation plays a central role: when poorly constrained, ^{10}Be concentrations tend to mirror accumulation variability (Yiou et al., 1985), complicating interpretations in terms of solar or geomagnetic modulation (Delaygue and Bard,

2011). Additional pre-depositional processes – such as stratospheric transport, volcanic injections (Baroni et al., 2011), wind-induced grain metamorphism (Lal et al., 2001), and general atmospheric aerosol dynamics (Zheng et al., 2024) – can all influence the ^{10}Be deposition. However, in the case presented here, we report distinct ^{10}Be minima that cannot be explained by variations in accumulation, deposition processes, or atmospheric circulation.

These ^{10}Be minima co-occur with sharp maxima in major ion concentrations (e.g., Na^+, Cl^-, Ca^{2+}), yet the ions originate from diverse sources. This rules out scenarios similar to single-source volcanic fallout (Baroni et al., 2011), terrestrial dust input (Baumgartner et al., 1997), or irregular snow redistribution (Poizat et al., 2024) and extreme atmospheric events such as atmospheric rivers (Wille et al., 2021). Instead, the inverse relationship between ^{10}Be and major ions suggests a post-depositional control. Spikes in the concentration of major ions have been observed in the deep section of EDC that had been linked to impurities migration in the ice crystal boundaries (Traversi et al., 2009). Anomalous ^{10}Be signals were also reported in the deepest parts of the EDC core (>700 ka; >3,100 m) (Raisbeck et al., 2006), documenting ^{10}Be maxima in EDC rather than minima as in TALDICE. This apparent contrast with TALDICE likely reflects differences in analytical protocols. In particular, the EDC study did not involve ion-exchange resin, unlike the present study. As reported in Kappelt et al. (2025), horizontal migration of Be was proposed to explain these maxima, as "smoothing over several thousands of years does not yield a distribution resembling the expected production signal smoothed by a vertical migration" (Kappelt et al., 2025). Under deep-ice conditions characterized by large grain sizes and enhanced impurity relocation, ^{10}Be may become incorporated into dust-rich aggregates or mineral phases at grain boundaries. Such particle-bound Be may not be quantitatively recovered by the ion-exchange protocol, leading to apparent ^{10}Be minima despite elevated concentrations of major ions. However, it is worth noting that some of the EDC ^{10}Be maxima were also concomitant with spikes in other species, including dust (Raisbeck et al., 2006). Similarly, major ion spikes in EDC were associated with low acidity (Raisbeck et al., 2006), which is different from the high acidity observed in TALDICE.

Baumgartner et al. (1997) proposed another mechanism to explain the covariations between ^{10}Be and dust. Indeed, in the deepest and warmest ice of the GRIP core (Greenland), up to 40–50 % of ^{10}Be become dust-bound – higher than the <5 % seen in Holocene ice – due to ice metamorphism. The migration of ^{10}Be and dusts at the ice grain boundaries would result in higher local concentrations and thus favour the adsorption of ^{10}Be onto dust particles. Although such effects are expected to be less pronounced in low-dust Antarctic settings, deeper sections of ice cores, where ice crystals are large, may promote localized enrichment of major ions and ^{10}Be adsorption onto grain-boundary dust, muting the dissolved-phase signal. This mechanism is also in agreement with higher relocations and reactions of dusts in deep TALDICE (Baccolo et al., 2021). The significant connection between ^{10}Be minima occurrence and elevated Ca^{2+} concentrations, particularly above 30 ppb, suggests that extreme, non-atmospheric conditions are the main drivers of these ^{10}Be minima. The absence of a significant relationship with the glacial/interglacial state, as defined by δD, reinforces the idea that these anomalies are not controlled by large-scale atmospheric changes in production or transport, but instead reflect in-ice processes. In this way, while further experimental work is needed to directly test this hypothesis, including stronger leaching protocols, ion remobilisation associated with ice

grain metamorphism, leading to ^{10}Be incorporation into larger mineral aggregates that are not released by our extraction protocol, provides a plausible mechanism for the observed ^{10}Be minima.

These short-scale ^{10}Be minima are typically confined to one or two consecutive samples representing 20 to 40 cm in depth, with only two events exceeding 60 cm. Their limited extent implies that the broader ^{10}Be flux record remains intact, preserving the long-term geomagnetic signal. In the TALDICE core, once these short-lived minima are accounted for and removed, the ^{10}Be record robustly mirror geomagnetic variability. Past studies had suggested to account for these outliers calculating a rolling median (Raisbeck et al., 2006). However, the median method results in similar ^{10}Be fluxes to those based on a rolling mean average (Figure S2). On average, the method based on minima identification results in +10 % ^{10}Be flux compared to the median method (Figure S2).

5.2 ^{10}Be ice core fluxes

Reconstructing ^{10}Be flux requires reliable estimates of both concentration and snow accumulation rate, as both parameters can vary by up to a factor of two during geomagnetic excursions or between glacial/interglacial variations, respectively. In particular, assessing snow accumulation rates across Termination III and MIS 7 is challenging, as this interval is marked by rapid and complex climatic variability (e.g., Caillon et al., 2003; Pérez-Mejías et al., 2017). This makes it essential to confirm the accuracy and precision of the accumulation reconstruction.

For the period 170–270 ka BP, the mean 3 ka rolling ^{10}Be flux in TALDICE, including the background and the geomagnetic events, is 1.44×10^5 at cm^{-2} a^{-1}, which slightly increases to 1.56×10^5 at cm^{-2} a^{-1} when the identified ^{10}Be minima are excluded. For the overlapping period 170–190 ka BP, the TALDICE ^{10}Be flux relative variations are in good agreement with the Dome Fuji (DF) record (Horiuchi et al., 2016) (Figure 4). This coherence not only highlights the homogeneous ^{10}Be deposition over East Antarctica, but also indicates that accumulation changes are well captured in both age models, AICC2023 for TALDICE (Bouchet et al., 2023) and the Dome Fuji DFO-2006 chronology (Kawamura et al., 2007). This agreement is further improved when the recent Dome Fuji chronology from Oyabu et al. (2022) is applied ($R^2 = 0.44$, with DF values calculated on TALDICE timestep), compared to the older DFO-2006 chronology ($R^2 = 0.37$). The consistent temporal evolution of ^{10}Be fluxes across these independent ice cores supports the reliability of these datasets for investigating variations in the GDM.

Despite this coherence in temporal evolution, DF exhibits systematically higher absolute ^{10}Be fluxes than TALDICE (c. 210 %, Figure 4). While the mean ^{10}Be flux in TALDICE is 1.56×10^5 at cm^{-2} a^{-1} over 170–190 ka BP (accounting for the minima), the DF ice core shows significantly higher values, reaching 2.74×10^5 at cm^{-2} a^{-1} (Horiuchi et al., 2016), or 2.68×10^5 at cm^{-2} a^{-1} when recalculated with the revised Dome Fuji chronology (Oyabu et al., 2022). The TALDICE values, however, are consistent with those from other Antarctic sites, such as EDC, which reports mean fluxes of approximately 1.44×10^5 at cm^{-2} a^{-1} for the period 200–300 ka BP (Cauquoin, 2013).

This pattern persists over the last millennium, between 918 and 1893 CE, the mean ^{10}Be flux was 1.64×10^5 at cm^{-2} a^{-1} at Dome C (Jouzel et al., 2026), and approximately twice as high at Dome Fuji (3.08×10^5 at cm^{-2} a^{-1}, Horiuchi et al., 2008). Although no ^{10}Be measurements are available for the last millennium at Talos Dome, comparison of recent century data shows

similar mean fluxes between Talos Dome (1.49×10^5 at cm^{-2} a^{-1}, Supplementary Table 1) and Dome C (1.69×10^5 at cm^{-2} a^{-1}, Jouzel et al., 2026). Independent evidence from the last millennium further indicates that Dome Fuji generally exhibits higher ^{10}Be fluxes than other East Antarctic sites. A recent multi-site compilation and modelling study (Jouzel et al., 2026) reports that measured ^{10}Be fluxes at Dome Fuji exceed those at EPICA Dome C by c. 70 %, consistent with earlier observations. These lower fluxes relative to the last millennium may be the results of the occurrence of solar minima during this interval corresponding to enhanced ^{10}Be production (Wolf, 1280 – 1350 CE; Spörer, 1420 – 1570 CE; Maunder 1645 – 1715 CE; Dalton 1790 – 1830 CE, Bard et al., 2000; Berggren et al., 2009; Horiuchi et al., 2008). These results suggest that persistent differences in ^{10}Be flux over Antarctica likely reflect regional deposition or atmospheric processes rather than artefacts of accumulation estimates or chronological treatment.

Jouzel et al. (2026) further suggest that this persistent contrast reflects regional atmospheric and depositional processes specific to the high-elevation interior of East Antarctica, including a transition from predominantly wet deposition north of 75°S to dry-dominated deposition south of this boundary, as well as enhanced stratosphere-troposphere exchanges over the highest Antarctic domes. While current global aerosol-climate models remain limited in their ability to resolve such sharp spatial gradients over Antarctica (Golubenko et al., 2024; Jouzel et al., 2026; Zheng et al., 2024), these mechanisms provide a physically grounded explanation for the systematically elevated ^{10}Be fluxes observed at Dome Fuji.

Importantly, we find no significant relationship between the Dome Fuji / TALDICE ^{10}Be flux ratio and δD (Spearman test, $p = 0.46$), indicating that differences in ^{10}Be flux over Antarctica is not modulated by glacial-interglacial climate variability. This result implies that the atmospheric and depositional mechanisms responsible for the DF/TALDICE ratio either remain stable through time or compensate one another across climate states. Consequently, while absolute ^{10}Be fluxes may differ between Antarctic sites, their relative temporal variations primarily reflect changes in cosmogenic production. This reinforces the use of Antarctic ice cores as robust records of global ^{10}Be production (modulo hemispheric polar bias; Adolphi et al., 2023) and supports their application to reconstruct variations in the geomagnetic dipole moment.

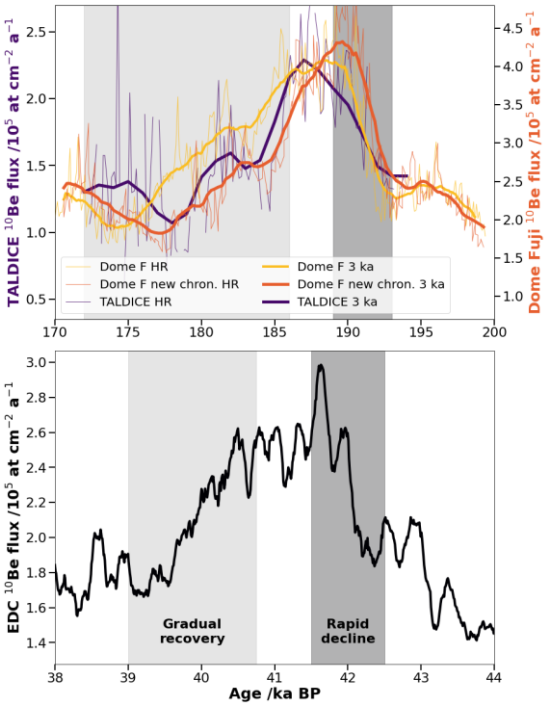

Figure 4: *Comparison of Dome Fuji (high resolution and 3 ka rolling mean average, yellow, Horiuchi et al., 2016) and TALDICE (purple, this study)* ^{10}*Be flux records for IBE. The revised Dome Fuji record is also presented based on chronology revision, which modifies snow accumulation rate (orange, Oyabu et al., 2022). The dark (resp. light) grey shaded area represents the period of rapid decline (resp. slow recovery) of the GDM. For comparison, the same periods can be identified during the Laschamps excursion in the* ^{10}*Be flux record from EPICA Dome C ice core* (Raisbeck et al., 2017)

5.3 Geomagnetic excursions between 170 ka BP and 270 ka BP

5.3.1 The low geomagnetic intensity during the Iceland Basin Excursion

The Iceland Basin Excursion (IBE), around 190 ka BP, stands out as one of the most prominent geomagnetic events during the Bruhnes chron (Simon et al., 2016). Based on the TALDICE ^{10}Be flux data, a flux enhancement factor of 1.59 to 2.08 is observed, depending on the reference background (see section 4. Results), similar to the twofold enhancement reported in Dome F (Horiuchi et al., 2016). In comparison, we calculate an enhancement ratio between 1.90 with the ^{10}Be flux calculated with the revised age of Dome Fuji, assuming a background calculated between 170 and 180 ka BP and a low-GDM plateau between 185.5 and 191 ka BP. Such ^{10}Be-based enhancement factors place IBE among the strongest known geomagnetic excursions of the last 1 Ma, comparable to the Laschamps event as measured in ^{10}Be in East Antarctic cores (Raisbeck et al., 2017) or authigenic ^{10}Be from oceanic cores (Simon et al., 2020), with no equivalent recorded between 200 and 800 ka BP (Cauquoin, 2013), and approaching the amplitude of the Bruhnes–Matuyama transition (Raisbeck et al., 2006; Simon et al., 2020). Assuming a constant solar modulation potential of 650 MV, ^{10}Be production scenarios can be calculated (Poluianov et

al., 2016) from the VADM reconstructions from RPI data (Channell et al., 2009) (Figure 5). For IBE peak, ^{10}Be production is expected to be 1.97 times higher than the 200 ka BP minimum ^{10}Be production according to the RPI-based VADM reconstruction (Channell et al., 2009), which is smaller than the observed 2.15 increase in the authigenic ^{10}Be/^{9}Be record (Figure 5, Simon et al., 2016).

Global transport models consistently indicate that polar ^{10}Be deposition originates from low-latitude production. GEOS-Chem simulations explicitly estimate deposition fluxes, indicating that about 52 % of ^{10}Be deposited between 60°S and 90°S is produced at lower latitudes (Zheng et al., 2024). As a result, a "polar bias" may affect ^{10}Be signals in Antarctic ice cores, as polar sites do not record solely polar atmospheric production but rather a mix between the ^{10}Be produced from low to high latitudes (Adolphi et al., 2023; Field et al., 2006). Model results suggest that geomagnetic field disturbances may be attenuated by 20 % to 37 % due to this bias under glacial conditions, but may not be attenuated during interglacial periods (Adolphi et al., 2023). Given that the IBE occurred during the interglacial MIS 7.1, the TALDICE ^{10}Be flux can be considered reliable for estimating enhancement factors. Accordingly, the observed twofold (2.08) flux increase at TALDICE would imply a complete depletion of the geomagnetic dipole moment, consistent with VADM reconstructions. Conversely, the lower factor of 1.59 would suggest either a smaller GDM reduction or a modest polar bias associated with the cooler conditions of MIS 7.1. This range reflects uncertainties in defining the background reference level, emphasizing the importance of background assumptions when quantifying excursion intensities from ^{10}Be flux records.

The structure of the ^{10}Be flux anomaly during IBE is also noteworthy. An asymmetric pattern, characterized by a rapid increase in ^{10}Be flux associated with dipole collapse followed by a slow and three-step dipole moment recovery was already identified in the Dome Fuji ice core record by Horiuchi et al., (2016) (Figure 4). Similar asymmetric dynamics have also been reported for the Laschamps excursion in ^{10}Be records from both ice cores (Muscheler et al., 2005; Raisbeck et al., 2017, Figure 4) and sediment cores (Ménabréaz et al., 2012; Simon et al., 2016, 2020). Interestingly, this asymmetric pattern is opposite, in a temporal sense, to that observed for polarity reversals (e.g., Valet and Meynadier, 1993; Valet et al., 2005): reversals are characterized by a slow decrease of the dipole moment in the initial polarity followed by an abrupt recovery of the dipole moment in the new opposite polarity. After long and intensive debates (Kok and Tauxe, 1996; Mazaud, 1996; Meynadier et al., 1998; Meynadier and Valet, 1996), the hypothesis was recently tested on authigenic ^{10}Be/^{9}Be records reconstructed from sediment cores (Simon et al., 2018; Valet et al., 2024, 2025) which suggested that the asymmetric patterns were not convincingly reproduced for any of the reversals of the last 4 Ma. However, the consistent asymmetry of the dipole moment collapse and recovery observed for Iceland Basin and Laschamps excursions might reveal a fundamental difference between the dynamics of excursions and reversals, and should be carefully considered in future geodynamo modeling efforts.

Regarding the timing, the IBE flux maximum forms a plateau between (192.07 ± 1.41) ka BP and (185.56 ± 1.44) ka BP, suggesting a ≈7 ka interval of extremely low magnetic field strength. This age is in general agreement with previous estimates from sedimentary and volcanic archives. For instance, the age aligns well with the K–Ar dating of transitional lava flows from the Snake River Plain at (188 ± 8) ka BP (Champion et al., 1988), and with excursion ages inferred from high-resolution marine sediment cores in the Ontong Java Plateau (≈190 ka BP; Tauxe and Wu, 1990) and the eastern equatorial Pacific (Valet and

Meynadier, 1993). It is also consistent with authigenic $^{10}Be/^{9}Be$ records from Portuguese margin cores (Carcaillet et al., 2004). Slightly older ages, such as the (197 ± 17) ka BP have been reported though for the Unzen lava flow in Japan (Shibuya et al., 2007). It should be noted that age uncertainties associated with both volcanic and sedimentary records are large, often of the same order as the reported differences between archives. Moreover, geomagnetic excursions associated with a collapse of the geomagnetic dipole moment are expected to be globally synchronous, as supported by cosmogenic nuclide records showing coherent ^{10}Be increases in both Greenland and Antarctic ice cores (Raisbeck et al., 2017). In this context, the spread in reported ages likely reflects the prolonged duration of the event, as indicated by the ≈7 ka plateau in ^{10}Be flux, which complicates the definition of a single "event age", combined with age uncertainties, rather than a true diachronism of the geomagnetic signal. Furthermore, fine-scale features in the IBE record, such as a short-lived recovery at 182 ka BP following a minimum at 183 ka BP, and a subsequent flux minimum around 178 ka BP with recovery by 174 ka BP, are visible in both TALDICE and DF cores as well as in oceanic cores (Figure 4). These well-resolved features are also mirrored in ocean sediment records (Black stars in Figure 5) and could serve as valuable tie points for synchronizing paleoclimate archives across different media. In contrast, the feature tentatively identified around c. 210 ka BP is less well constrained and should be regarded as having a higher uncertainty in its assignment.

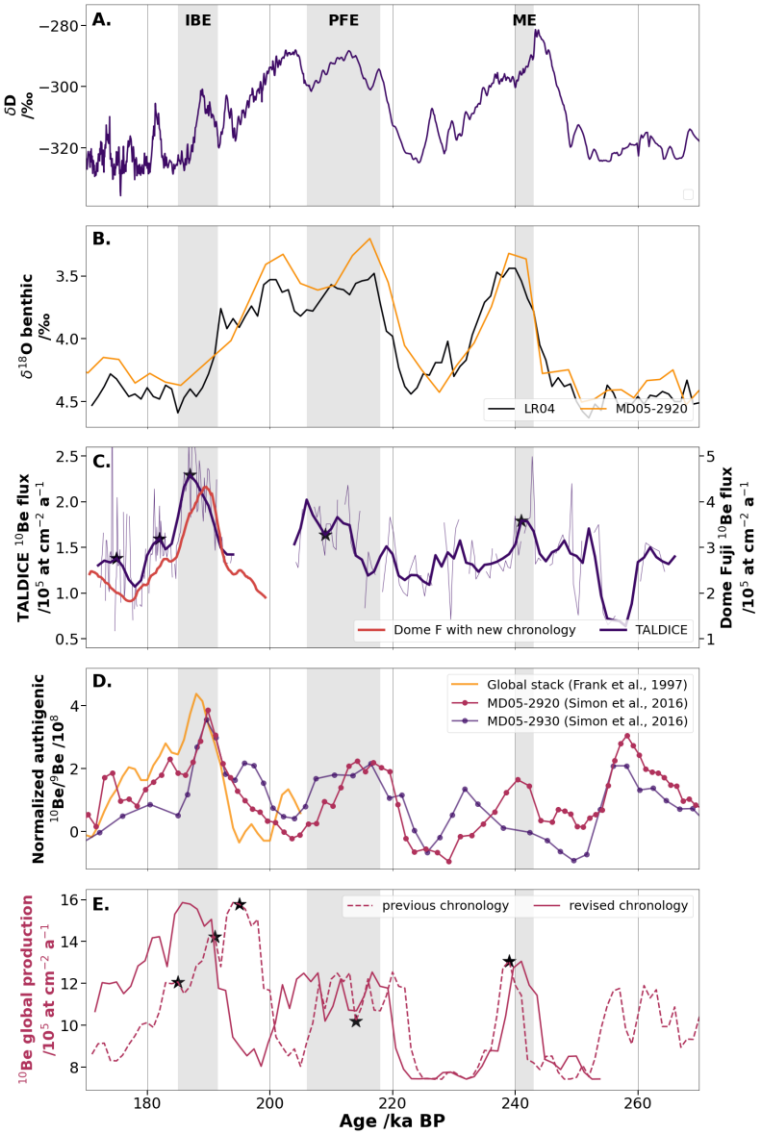

***Figure 5**: Comparison of ^{10}Be and climate records from ice cores and marine sediments over 170–270 ka BP with: A. TALDICE δD (/‰), B. benthic δ^{18}O (/‰) from LR04 stack (Lisiecki and Raymo, 2005) and MD05-2920 (Tachikawa et al., 2014), C. TALDICE and Dome Fuji ^{10}Be (in purple and red respectively, /at cm^{-2} a^{-1}), D. authigenic ^{10}Be/^{9}Be from global stack reconstruction (yellow, Frank et al., 1997), MD05-2920 (red), and MD05-2932 (purple) (Simon et al., 2016), and E. the ^{10}Be global production (/at cm^{-2} a^{-1}; Poluianov et al., 2016) calculated from RPI-based VADM (Channell et al., 2009). Grey bars highlight the main geomagnetic excursions discussed in the text (IBE, PFE, ME). Timing of identifiable geomagnetic features (black stars in TALDICE and RPI-based VADM) is used to obtain a revised chronology of RPI-based VADM used for calculating the ^{10}Be production, noting though a lower confidence on the star around 210 ka BP.*

5.3.2 The lower amplitude Pringle Falls and Mamaku Excursions

In addition to the IBE, the TALDICE ^{10}Be record supports the existence of two distinct geomagnetic events for the period 205-270 ka BP (Figure 5). The identification of lower-amplitude geomagnetic excursions in this interval requires a cautious approach (see section 2.2 and Channell et al., 2020). Unlike more prominent events, these excursions often lack clear and well-dated signatures. The first event, occurring between (206.0 ± 0.8) ka BP and (218.5 ± 1.9) ka BP, shows a flux enhancement factor of 1.24 or 1.62, depending on the background reference, and is here associated with the Pringle Falls Excursion (PFE). The second, centred at (242.0 ± 0.3) ka BP, shows a peak enhancement factor of 1.25 or 1.63, and is tentatively identified as the Mamaku Excursion (ME). To the best of our knowledge, it is the first discussion of these events in an ice core. Compared with the authigenic ^{10}Be/^{9}Be record (Simon et al., 2016), TALDICE ^{10}Be flux suggests that the PFE and ME are of similar moderate amplitude but differing in duration: the PFE is characterized by a prolonged period (≈8 ka) of reduced field intensity, while the ME presents a brief minimum lasting only 2–3 ka, in agreement with PISO-1500 variations (Channell et al., 2009). Around 232 ka BP, a maximum in authigenic ^{10}Be/^{9}Be in MD05-2930 is observed. However, as this feature is not clearly reproduced in other marine records or in TALDICE ^{10}Be flux, we do not assign a geomagnetic origin to this signal.

Variations in ^{10}Be flux are more directly representative of changes in cosmogenic production, unlike ^{10}Be concentrations which are strongly modulated by snow accumulation. In this context, it is noteworthy that, unlike the IBE, the PFE and ME are not clearly expressed in ^{10}Be concentrations, and only emerge in the ^{10}Be flux (i.e., once considering snow accumulation rate variations and considering ^{10}Be minima). This raises the possibility whether these low-amplitude signals could be artifacts related to accumulation-rate variations or age-model uncertainties. Nevertheless, both events occur during interstadial periods (MIS 7.3 for PFE and MIS 7.5 for ME) marked by elevated accumulation rates, approximately 8 cm a^{-1} (Figure 2), thus supporting the consideration of snow accumulation rate variations. This is further corroborated by the correlation between the concentrations of Na^{+} and ^{10}Be (R^2 = 0.23, after the removal of the minima, Figure S3) which indicates that about 23 % of ^{10}Be concentration is explained by climate-driven variations in ^{10}Be deposition. Moreover, the robustness of the AICC2023 chronology over this interval, supported by a dense network chronostratigraphic markers (Bouchet et al., 2023), strengthens the reliability of the flux signals. While confirmation from additional ice cores is required, the present evidence supports the occurrence of two distinct moderate geomagnetic excursions (PFE and ME), enriching the geomagnetic field history during MIS 7. This observation further emphasizes that relying solely on ^{10}Be concentrations may lead to biased interpretations of ^{10}Be production when glacial and interglacial periods alternate, and that both ^{10}Be concentrations and snow accumulation rates should be reported to allow robust geomagnetic interpretations.

The relatively modest amplitude of the Pringle Falls and Mamaku excursions raises the question of whether their visibility in the TALDICE ^{10}Be record could be enhanced by climatic conditions, beyond a bias resulting from snow accumulation reconstruction. In particular, the occurrence of the three excursions during warm interstadial substages of MIS 7 (7.1 for IBE, 7.3 for PFE, and 7.5 for ME), i.e., relatively warm intervals within MIS7, raises the question of a climate-dependent polar bias. Model studies suggest that polar ^{10}Be records are less sensitive to geomagnetic field variations under glacial conditions, when

atmospheric mixing is reduced, and more responsive under interglacial climates (Adolphi et al., 2023). In this view, excursions expressed during interglacials may partly reflect enhanced transmission of the global ^{10}Be production signal to polar deposition, while equivalent geomagnetic variations during glacial periods would appear more attenuated. However, the polar bias affects amplitude rather than timing: it cannot generate spurious excursions, but may modulate their visibility in ice core records. The consistent expression of IBE, PFE, and ME in both ice and marine archives, including RPI, indicates that these events correspond to genuine geomagnetic disturbances, albeit potentially amplified by more efficient atmospheric mixing during interglacials.

A further event around 258–262 ka BP has been reported in marine records, including a pronounced ^{10}Be/^{9}Be peak in equatorial Pacific sediments (Simon et al., 2016) and RPI lows in Atlantic and Mediterranean archives (Langereis et al., 1997; Lund et al., 2001; Nowaczyk and Frederichs, 1999). This excursion, sometimes termed the Calabrian Ridge 0, 8α, or Fram Strait event, is not expressed in TALDICE (Figure 5). Its absence can be explained by the fact that this interval coincides with long-lasting ^{10}Be low values, which cannot be identified as minima by our statistical filtering procedure, preventing detection of a robust flux signal. Additional high-resolution ice core data will be required to evaluate whether this excursion can be identified in Antarctic records.

5.4 Consistency of ice core and oceanic ^{10}Be records

The comparison between atmospheric ^{10}Be fluxes from ice cores and authigenic ^{10}Be/^{9}Be ratios from marine sediments reveals overall agreement (Figure S4.A), supporting the reliability of both archives in recording geomagnetic events. Previous studies have highlighted the close correspondence between atmospheric and authigenic ^{10}Be records (e.g., Czymzik et al., 2020; Horiuchi et al., 2016). For IBE, high-resolution alignment is observed between ice cores (TALDICE and Dome Fuji, see section 5.3.1) and marine sediment cores (Figure 5). In particular, MD05-2920 (Simon et al., 2016) and KR0515-PC2 (Horiuchi et al., 2016) captures the same three ^{10}Be peaks at 174, 182, and 187 ka BP. PFE is also identified in both MD05-2920 and MD05-2930, while ME is not detected in MD05-2930, likely due to the core's lower temporal resolution (ca. 4 ka around 240 ka BP), which may not resolve the short 2–3 ka duration of the event.

A systematic time offset between the oceanic and the ice core records is observed (Figures 5, S4.A). A similar 3 to 4.5 ka offset between oceanic and Dome F ice core records was previously reported by Horiuchi et al., (2016), and interpreted it primarily in terms of magnetic lock-in depth associated with post-depositional remanent magnetization acquisition in marine sediments. Our results confirm the existence of a comparable offset using independent marine and ice core datasets, but extend the comparison to ice core ^{10}Be fluxes, which are not affected by magnetization processes. When comparing authigenic ^{10}Be/^{9}Be from core MD05-2920 to the TALDICE ^{10}Be flux, the best correlation is obtained when the oceanic record is shifted 3 ka younger (R^2 = 0.37, Figure S4), which remains within the uncertainties of the marine core age model (Tachikawa et al., 2014). Unlike comparisons involving RPI, a phase shift between ice core and oceanic ^{10}Be records cannot be attributed to magnetic lock-in effects. Potential physical causes would instead involve atmospheric or oceanic transport and mixing

processes. Nevertheless, does this 3-ka offset result from age model uncertainties or reflect a physical lag in the system, thereby limiting the possibility to use paleomagnetic events as chronostratigraphic horizons?

A phase shift linked to mixing processes would result in a delayed and attenuated ^{10}Be signal. Although excursion amplitudes are consistent between the two archives (Figure 5), this depends on complex processes that can be involved such as polar bias linked to incomplete atmospheric mixing (Adolphi et al., 2023), oceanic circulation and transport (Jeromson et al., 2025; Savranskaia et al., 2021) and bioturbation in sediments (Raisbeck et al., 1985). Nevertheless, if a physical phase shift occurred, we would expect the ice core signal to lead the oceanic record due to various oceanic mixing effects, thereby resulting in a delayed (and attenuated) marine authigenic ^{10}Be/^{9}Be signal.

To investigate the delay, we can examine the cross-correlation between the ^{10}Be/^{9}Be from core MD05-2920 and the ^{10}Be flux from TALDICE, similar to the approach of Horiuchi et al., (2016). Such analysis (Figure S4.B) shows the highest correlation when MD05-2920 is shifted by 3 to 3.7 ka earlier. Another approach consists in examining the evolution of the delay between well-defined paleomagnetic events identified in both records (marked with stars in Figure 5). If major changes in oceanic circulation influenced the sedimentation of oceanic ^{10}Be, the lag would vary between glacial and interglacial periods (Savranskaia et al., 2024). However, we observe no variation in the lag across glacial–interglacial variations (Figure S4.C), indicating a consistent phase relationship between atmospheric and authigenic ^{10}Be signals. This approach yields a mean offset of 2.3 ka (Figure S4.C). Taken together, these results suggest that the observed delay is the result of age model uncertainty in the marine core, and that ^{10}Be production events are likely recorded synchronously in both oceanic and ice core archives. This conclusion is consistent with previous findings that suggest a limited reservoir effect and minimal climatic bias in ^{10}Be-based chronologies (Ménabréaz et al., 2012). These findings reinforce the value of ^{10}Be as a reliable synchronizing tool across sediment and ice archives. In the context of the Beyond EPICA project, they emphasize the role of ^{10}Be in refining chronologies and investigating climatic transitions, particularly across complex intervals such as the Mid-Pleistocene Transition (1.2 – 0.9 Ma, Fischer et al., 2013; Parrenin et al., 2017; Wolff et al., 2022).

During IBE, the TALDICE ^{10}Be flux record closely follows variations in oceanic authigenic ^{10}Be/^{9}Be from a global compilation (Frank et al., 1997) (Figure 5). In particular, the timing, duration, and stepped structure of the collapse and subsequent recovery of the GDM are consistent between the ice cores and marine records (Figure 5). For instance, the ≈7 ka plateau of elevated ^{10}Be flux observed in TALDICE has also been observed in Dome F ice core (Horiuchi et al., 2016) and is in agreement with oceanic records (Knudsen et al., 2008). Besides, the good overall agreement between the TALDICE and Dome F records with global geomagnetic field model of the IBE (Lanci et al., 2008) further supports the global record of Antarctic ice cores.

Because of this broad global agreement, a comparison of ^{10}Be production calculated from RPI-based VADM and authigenic ^{10}Be/^{9}Be with ice core ^{10}Be fluxes is possible. Using the VADM reconstruction PISO-1500 (Channell et al., 2009) and assuming a constant solar modulation potential of 650 MV, ^{10}Be production was calculated following Poluianov et al. (2016). Between 170 and 270 ka BP, ^{10}Be production was at a mean of 10.5×10^5 at cm^{-2} a^{-1} (min = 7.4 ; max = 15.9). Compared with the 1.56×10^5 at cm^{-2} a^{-1} mean flux in TALDICE (removing ^{10}Be minima), this reveals a mean scaling factor of 6.7 (min =

4.8; max = 10.2). This scaling factor reflects the combined influence of geographic production patterns, including hemispheric asymmetries in production (Panovska et al., 2023) and atmospheric transport and deposition (Delaygue and Bard, 2011; Golubenko et al., 2024; Heikkilä et al., 2009). Consequently, quantitative interpretation of these ratios remains difficult, which highlights the need for continued model/data integration to constrain transport and deposition processes.

6 Synthesis and conclusion

This study presents a high-resolution ^{10}Be flux record from the East Antarctic TALDICE ice core, covering the interval from 170 to 270 ka BP, and evaluates the reliability of ^{10}Be as a paleomagnetic proxy and as a tool for synchronizing the chronologies of different proxy archives. Three main conclusions emerge:

1. **Identification of ^{10}Be minima**

Within our record, 52 ^{10}Be minima restricted to single or double sample layers have been identified, most coinciding with maxima in major ion concentrations. Such observation indicate that these minima are likely the result of post-depositional processes within the ice rather than changes in atmospheric production. Although the precise mechanism remains unresolved, these minima were identified, and, once corrected for, did not compromise the reliability of the geomagnetic signal. Future high-resolution analytical approaches, such as laser ablation, may help quantify the redistribution of impurities in old ice crystals, thereby enabling the mechanisms of ^{10}Be redistribution to be identified. In the quest of old ice samples, such investigations will be particularly important for interpreting highly-rearranged ice layers in deep or blue ice records, and call for improved extraction protocols that take in-ice remobilization into account.

2. **Recording the geomagnetic dipole moment variations**

The TALDICE record demonstrates clear preservation of high-amplitude geomagnetic excursions, but also smaller ones, first identified in an ice core. The Iceland Basin Excursion (IBE) is well recorded, with a flux enhancement factor of 1.59–2.08 and a clearly defined low-dipole field interval between (192.0 ± 1.4) ka BP and (185.6 ± 1.4) ka BP. The structure of this event is notably asymmetrical, with a rapid decline in dipole intensity followed by a more gradual, three-step recovery, and may highlight fundamental differences between excursion and reversal dynamics, with implications for geodynamo modeling.

In addition to the geodynamo physics, the IBE is a valuable analogue of the Laschamps excursion, providing an opportunity to reassess the proposed modifications in atmospheric processes suggested for the Laschamps event. For instance, the prolonged low dipole field and its potential impact on atmospheric chemistry and biological systems (e.g., Cooper et al., 2021; Dasari et al., 2022) make it a prime target for future interdisciplinary investigations.

In addition, the TALDICE ^{10}Be record captures two lower-amplitude geomagnetic excursions: a long-lasting Pringle Falls Excursion (PFE), from (218.5 ± 1.9) to (206.0 ± 0.8) ka BP, and a brief Mamaku Excursion (ME) at (242.0 ± 0.3) ka BP, both associated with flux enhancement factors of 1.24 to 1.63. However, the 258–262 ka BP excursion is not observed in TALDICE due to prolonged ^{10}Be minima values and a gap in the dataset. Nevertheless, the observation of small amplitude features in the records, including the three step IBE recovery and the PFE and ME, offer great possibility for cross-checking the chronologies of different archives.

3. Agreement between oceanic and ice core records

The strong agreement between TALDICE and marine authigenic $^{10}Be/^{9}Be$ records reinforces the potential of ^{10}Be as a robust tool for synchronizing marine and ice core archives.

Our results reveal that the oceanic records (MD05-2920 and MD05-2930) precede the ice core by ca. 3 ka, a discrepancy attributable to uncertainties in the age model rather than a genuine phase shift. Crucially, no systematic differences were observed between glacial and interglacial intervals, which further validates the limited oceanic-atmospheric differences. This multi-archive consistency not only strengthens the fidelity of reconstructions of past geomagnetic dipole moment variations, but also offers a promising avenue for refining chronologies and exploring climate-magnetic field interactions during critical intervals such as the Mid-Pleistocene Transition.

Data availability

A Zenodo repository is available with the following dataset (Lamothe et al., 2025):

Sheet 1: Depth top, depth bottom, Age top from AICC2023, age bottom, age uncertainty, accumulation, accumulation uncertainty, Be concentration, Be concentration uncertainty, Be flux, Be flux uncertainty

Sheet 2: Depth, concentration of major ions (Cl^-, $CH_3SO_3^-$ (MSA), F^-, NO_3^-, SO_4^{2-}, Na^+, NH_4^+, K^+, Mg^{2+}, and Ca^{2+}).

Author contributions

AL and MB conceptualized the study. Formal analysis was performed by AL, EA, MS, RT, MA, FW, RM, KK, GA, and FZ. Investigation and validation was done by AL, EB, NT, and MB. MB managed the project and aquired the funding. AL was supervised by MB and EB. AL undertook data curation, visualization, and writing of the first draft, with contributions from all co-authors.

Conflict of interests

The authors have no conflicts of interest to declare.

Acknowledgements

This publication benefited from the funding of the ANR project ToBE (ANR-22-CE01-0024). This publication was generated in the frame of Beyond EPICA. The project has received funding from the European Union's Horizon 2020 research and innovation program under grant agreement nos. 730258 (Oldest Ice) and 815384 (Oldest Ice Core). It is supported by national partners and funding agencies in Belgium, Denmark, France, Germany, Italy, Norway, Sweden, Switzerland, the Netherlands and the United Kingdom. Logistic support is mainly provided by ENEA and IPEV through the Concordia Station system.

The Talos Dome Ice core Project (TALDICE), a joint European program, is funded by national contributions from Italy, France, Germany, Switzerland and the United Kingdom. Primary logistical support was provided by PNRA at Talos Dome. ^{10}Be measurements were performed at ASTER AMS, as part of the Laboratoire National des Nucléides Cosmogéniques (LN2C) national platform (CEREGE, Aix-en-Provence, https://www.cerege.fr/en/equipment/laboratoire-national-des-nucleides-cosmogeniques/ams-aster/), which is supported by the INSU/CNRS and IRD, and member of Aix- Marseille Platforms and REGEF networks.

We deeply thank all collaborators. We would like to express our sincere gratitude to Stepan Poluianov and Ilya Usoskin for generously sharing their atmospheric cosmonuclide production model with us. We thank Patrick Ginot and Bruno Jourdain for their dedicated time to the ion chromatography measurements at IGE. We thank the TALDICE logistic and drilling team. We thank Marie Bouchet for her discussion on the uncertainty in the accumulation. We thank the engineers of the Laboratoire de géochimie organique, inorganique et isotopique (LGO2i) platform (https://www.cerege.fr/en/equipment/technical-clusters/geochemistry-organic-inorganic-and-isotopic-2/), Frauke Rostek, Thibault Tuna, and Yoann Fagault. We thank the administrative and IT support teams from CEREGE. We thank the NJS Faramia cold storage facility. We used AI tools (Deepl and ChatGPT) to help us refine our English.

This is TALDICE publication n°XX. This is Beyond Epica publication n°XX.

References

Adolphi, F., Herbst, K., Nilsson, A., and Panovska, S.: On the Polar Bias in Ice Core 10Be Data, Journal of Geophysical Research: Atmospheres, 128, e2022JD038203, https://doi.org/10.1029/2022JD038203, 2023.

Arnold, M., Merchel, S., Bourlès, D. L., Braucher, R., Benedetti, L., Finkel, R. C., Aumaître, G., Gottdang, A., and Klein, M.: The French accelerator mass spectrometry facility ASTER: Improved performance and developments, Nuclear Instruments and Methods in Physics Research Section B: Beam Interactions with Materials and Atoms, 268, 1954–1959, https://doi.org/10.1016/j.nimb.2010.02.107, 2010.

Baccolo, G., Delmonte, B., Niles, P. B., Cibin, G., Di Stefano, E., Hampai, D., Keller, L., Maggi, V., Marcelli, A., Michalski, J., Snead, C., and Frezzotti, M.: Jarosite formation in deep Antarctic ice provides a window into acidic, water-limited weathering on Mars, Nat Commun, 12, 436, https://doi.org/10.1038/s41467-020-20705-z, 2021.

Bard, E., Raisbeck, G., Yiou, F., and Jouzel, J.: Solar irradiance during the last 1200 years based on cosmogenic nuclides, Tellus B, 52, 985–992, https://doi.org/10.1034/j.1600-0889.2000.d01-7.x, 2000.

Baroni, M., Bard, E., Petit, J.-R., Magand, O., and Bourlès, D.: Volcanic and solar activity, and atmospheric circulation influences on cosmogenic 10Be fallout at Vostok and Concordia (Antarctica) over the last 60 years, Geochimica et Cosmochimica Acta, 75, 7132–7145, https://doi.org/10.1016/j.gca.2011.09.002, 2011.

Baumgartner, S., Beer, J., Wagner, G., Kubik, P., Suter, M., Raisbeck, G. M., and Yiou, F.: 10Be and dust, Nuclear Instruments and Methods in Physics Research Section B: Beam Interactions with Materials and Atoms, 123, 296–301, https://doi.org/10.1016/S0168-583X(96)00751-3, 1997.

Berggren, A.-M., Beer, J., Possnert, G., Aldahan, A., Kubik, P., Christl, M., Johnsen, S. J., Abreu, J., and Vinther, B. M.: A 600-year annual 10Be record from the NGRIP ice core, Greenland, Geophysical Research Letters, 36, https://doi.org/10.1029/2009GL038004, 2009.

Bono, R. K., Paterson, G. A., and Biggin, A. J.: MCADAM: A Continuous Paleomagnetic Dipole Moment Model for at Least 3.7 Billion Years, Geophysical Research Letters, 49, e2022GL100898, https://doi.org/10.1029/2022GL100898, 2022.

Bouchet, M., Landais, A., Grisart, A., Parrenin, F., Prié, F., Jacob, R., Fourré, E., Capron, E., Raynaud, D., Lipenkov, V. Y., Loutre, M.-F., Extier, T., Svensson, A., Legrain, E., Martinerie, P., Leuenberger, M., Jiang, W., Ritterbusch, F., Lu, Z.-T., and Yang, G.-M.: The Antarctic Ice Core Chronology 2023 (AICC2023) chronological framework and associated timescale for the European Project for Ice Coring in Antarctica (EPICA) Dome C ice core, Climate of the Past, 19, 2257–2286, https://doi.org/10.5194/cp-19-2257-2023, 2023.

Braucher, R., Guillou, V., Bourlès, D. L., Arnold, M., Aumaître, G., Keddadouche, K., and Nottoli, E.: Preparation of ASTER in-house 10Be/9Be standard solutions, Nuclear Instruments and Methods in Physics Research Section B: Beam Interactions with Materials and Atoms, 361, 335–340, https://doi.org/10.1016/j.nimb.2015.06.012, 2015.

Caillon, N., Severinghaus, J. P., Jouzel, J., Barnola, J.-M., Kang, J., and Lipenkov, V. Y.: Timing of atmospheric CO2 and Antarctic temperature changes across Termination III, Science, 299, 1728–1731, 2003.

Carcaillet, J., Bourlès, D. L., Thouveny, N., and Arnold, M.: A high resolution authigenic 10Be/9Be record of geomagnetic moment variations over the last 300 ka from sedimentary cores of the Portuguese margin, Earth and Planetary Science Letters, 219, 397–412, https://doi.org/10.1016/S0012-821X(03)00702-7, 2004.

Cauquoin, A.: Flux de 10Be en Antarctique durant les 800 000 dernières années et interprétation, phdthesis, Université Paris Sud - Paris XI, 2013.

Champion, D. E., Dalrymple, G. B., and Kuntz, M. A.: Radiometric and paleomagnetic evidence for the Emperor reversed polarity event at 0.46 ± 0.05 M.Y. in basalt lava flows from the eastern Snake River Plain, Idaho, Geophysical Research Letters, 8, 1055–1058, https://doi.org/10.1029/GL008i010p01055, 1981.

Champion, D. E., Lanphere, M. A., and Kuntz, M. A.: Evidence for a new geomagnetic reversal from Lava flows in Idaho: Discussion of short polarity reversals in the Brunhes and late Matuyama polarity chrons, Journal of Geophysical Research: Solid Earth, 93, 11667–11680, https://doi.org/10.1029/JB093iB10p11667, 1988.

Channell, J.: Late Brunhes polarity excursions (Mono Lake, Laschamp, Iceland Basin and Pringle Falls) recorded at ODP Site 919 (Irminger Basin), Earth and Planetary Science Letters, 244, 378–393, https://doi.org/10.1016/j.epsl.2006.01.021, 2006.

Channell, J. E. T.: Geomagnetic paleointensity and directional secular variation at Ocean Drilling Program (ODP) Site 984 (Bjorn Drift) since 500 ka: Comparisons with ODP Site 983 (Gardar Drift), Journal of Geophysical Research: Solid Earth, 104, 22937–22951, https://doi.org/10.1029/1999JB900223, 1999.

Channell, J. E. T.: The Iceland Basin excursion: Age, duration, and excursion field geometry, Geochemistry, Geophysics, Geosystems, 15, 4920–4935, https://doi.org/10.1002/2014GC005564, 2014.

Channell, J. E. T. and Raymo, M. E.: Paleomagnetic record at ODP Site 980 (Feni Drift, Rockall) for the past 1.2 Myrs, Geochemistry, Geophysics, Geosystems, 4, https://doi.org/10.1029/2002GC000440, 2003.

Channell, J. E. T., Hodell, D. A., and Lehman, B.: Relative geomagnetic paleointensity and d18O at ODP Site 983 (Gardar Drift, North Atlantic) since 350 ka, Earth and Planetary Science Letters, 153, 103–118, 1997.

Channell, J. E. T., Xuan, C., and Hodell, D. A.: Stacking paleointensity and oxygen isotope data for the last 1.5 Myr (PISO-1500), Earth and Planetary Science Letters, 283, 14–23, https://doi.org/10.1016/j.epsl.2009.03.012, 2009.

Channell, J. E. T., Hodell, D. A., and Curtis, J. H.: ODP Site 1063 (Bermuda Rise) revisited: Oxygen isotopes, excursions and paleointensity in the Brunhes Chron, Geochemistry, Geophysics, Geosystems, 13, https://doi.org/10.1029/2011GC003897, 2012.

Channell, J. E. T., Singer, B. S., and Jicha, B. R.: Timing of Quaternary geomagnetic reversals and excursions in volcanic and sedimentary archives, Quaternary Science Reviews, 228, 106114, https://doi.org/10.1016/j.quascirev.2019.106114, 2020.

Chmeleff, J., Von Blanckenburg, F., Kossert, K., and Jakob, D.: Determination of the 10Be half-life by multicollector ICP-MS and liquid scintillation counting, Nuclear Instruments and Methods in Physics Research Section B: Beam Interactions with Materials and Atoms, 268, 192–199, https://doi.org/10.1016/j.nimb.2009.09.012, 2010.

Christl, M., Lippold, J., Steinhilber, F., Bernsdorff, F., and Mangini, A.: Reconstruction of global 10Be production over the past 250ka from highly accumulating Atlantic drift sediments, Quaternary Science Reviews, 29, 2663–2672, https://doi.org/10.1016/j.quascirev.2010.06.017, 2010.

Chung, A., Parrenin, F., Mulvaney, R., Vittuari, L., Frezzotti, M., Zanutta, A., Lilien, D. A., Cavitte, M. G. P., and Eisen, O.: Age, thinning and spatial origin of the Beyond EPICA ice from a 2.5D ice flow model, The Cryosphere, 19, 4125–4140, https://doi.org/10.5194/tc-19-4125-2025, 2025.

Cooper, A., Turney, C. S. M., Palmer, J., Hogg, A., McGlone, M., Wilmshurst, J., Lorrey, A. M., Heaton, T. J., Russell, J. M., McCracken, K., Anet, J. G., Rozanov, E., Friedel, M., Suter, I., Peter, T., Muscheler, R., Adolphi, F., Dosseto, A., Faith, J. T., Fenwick, P., Fogwill, C. J., Hughen, K., Lipson, M., Liu, J., Nowaczyk, N., Rainsley, E., Bronk Ramsey, C., Sebastianelli, P., Souilmi, Y., Stevenson, J., Thomas, Z., Tobler, R., and Zech, R.: A global environmental crisis 42,000 years ago, Science, 371, 811–818, https://doi.org/10.1126/science.abb8677, 2021.

Crotti, I., Landais, A., Stenni, B., Bazin, L., Parrenin, F., Frezzotti, M., Ritterbusch, F., Lu, Z.-T., Jiang, W., Yang, G.-M., Fourré, E., Orsi, A., Jacob, R., Minster, B., Prié, F., Dreossi, G., and Barbante, C.: An extension of the TALDICE ice core age scale reaching back to MIS 10.1, Quaternary Science Reviews, 266, 107078, https://doi.org/10.1016/j.quascirev.2021.107078, 2021.

Czymzik, M., Nowaczyk, N. R., Dellwig, O., Wegwerth, A., Muscheler, R., Christl, M., and Arz, H. W.: Lagged atmospheric circulation response in the Black Sea region to Greenland Interstadial 10, Proceedings of the National Academy of Sciences, 117, 28649–28654, https://doi.org/10.1073/pnas.2005520117, 2020.

Dasari, S., Paris, G., Charreau, J., and Savarino, J.: Sulfur-isotope anomalies recorded in Antarctic ice cores as a potential proxy for tracing past ozone layer depletion events, PNAS Nexus, 1, pgac170, https://doi.org/10.1093/pnasnexus/pgac170, 2022.

Delaygue, G. and Bard, E.: An Antarctic view of Beryllium-10 and solar activity for the past millennium, Clim Dyn, 36, 2201–2218, https://doi.org/10.1007/s00382-010-0795-1, 2011.

Demory, F., Nowaczyk, N. R., Witt, A., and Oberhänsli, H.: High-resolution magnetostratigraphy of late quaternary sediments from Lake Baikal, Siberia: timing of intracontinental paleoclimatic responses, Global and Planetary Change, 46, 167–186, https://doi.org/10.1016/j.gloplacha.2004.09.016, 2005.

Evans, H. F., Channell, J. E. T., Stoner, J. S., Hillaire-Marcel, C., Wright, J. D., Neitzke, L. C., and Mountain, G. S.: Paleointensity-assisted chronostratigraphy of detrital layers on the Eirik Drift (North Atlantic) since marine isotope stage 11, Geochemistry, Geophysics, Geosystems, 8, https://doi.org/10.1029/2007GC001720, 2007.

Field, C. V., Schmidt, G. A., Koch, D., and Salyk, C.: Modeling production and climate-related impacts on 10Be concentration in ice cores, Journal of Geophysical Research: Atmospheres, 111, https://doi.org/10.1029/2005JD006410, 2006.

Fischer, H., Severinghaus, J., Brook, E., Wolff, E., Albert, M., Alemany, O., Arthern, R., Bentley, C., Blankenship, D., Chappellaz, J., Creyts, T., Dahl-Jensen, D., Dinn, M., Frezzotti, M., Fujita, S., Gallee, H., Hindmarsh, R., Hudspeth, D., Jugie, G., Kawamura, K., Lipenkov, V., Miller, H., Mulvaney, R., Parrenin, F., Pattyn, F., Ritz, C., Schwander, J., Steinhage, D., van Ommen, T., and Wilhelms, F.: Where to find 1.5 million yr old ice for the IPICS "Oldest-Ice" ice core, Climate of the Past, 9, 2489–2505, https://doi.org/10.5194/cp-9-2489-2013, 2013.

Frank, M., Schwarz, B., Baumann, S., Kubik, P. W., Suter, M., and Mangini, A.: A 200 kyr record of cosmogenic radionuclide production rate and geomagnetic field intensity from 10Be in globally stacked deep-sea sediments1, Earth and Planetary Science Letters, 149, 121–129, https://doi.org/10.1016/S0012-821X(97)00070-8, 1997.

Frezzotti, M., Bitelli, G., Michelis, P. D., Deponti, A., Forieri, A., Gandolfi, S., Maggi, V., Mancini, F., Remy, F., Tabacco, I. E., Urbini, S., Vittuari, L., and Zirizzottl, A.: Geophysical survey at Talos Dome, East Antarctica: the search for a new deep-drilling site, Annals of Glaciology, 39, 423–432, https://doi.org/10.3189/172756404781814591, 2004.

Gee, J. S., Cande, S. C., Hildebrand, J. A., Donnelly, K., and Parker, R. L.: Geomagnetic intensity variations over the past 780 kyr obtained from near-seafloor magnetic anomalies, Nature, 408, 827–832, https://doi.org/10.1038/35048513, 2000.

Geissman, J. W., Brown, L., Turrin, B. D., Mcfadden, L. D., and Harlan, S. S.: Brunhes chron excursion/polarity episode recorded during the late pleistocene, Albuquerque Volcanoes, New Mexico, USA, Geophysical Journal International, 102, 73–88, https://doi.org/10.1111/j.1365-246X.1990.tb00531.x, 1990.

Gissinger, C.: A new deterministic model for chaotic reversals, Eur. Phys. J. B, 85, 137, https://doi.org/10.1140/epjb/e2012-20799-5, 2012.

Golubenko, K., Rozanov, E., Kovaltsov, G., and Usoskin, I.: Zonal Mean Distribution of Cosmogenic Isotope (7Be, 10Be, 14C, and 36Cl) Production in Stratosphere and Troposphere, Journal of Geophysical Research: Atmospheres, 127, e2022JD036726, https://doi.org/10.1029/2022JD036726, 2022.

Golubenko, K., Rozanov, E., Kovaltsov, G., Baroni, M., Sukhodolov, T., and Usoskin, I.: Full Modeling and Practical Parameterization of Cosmogenic 10Be Transport for Cosmic-Ray Studies: SOCOL-AERv2-BE Model, Journal of Geophysical Research: Space Physics, 129, e2024JA032504, https://doi.org/10.1029/2024JA032504, 2024.

Guyodo, Y. and Valet, J.-P.: Relative variations in geomagnetic intensity from sedimentary records: the past 200,000 years, Earth and Planetary Science Letters, 143, 23–36, https://doi.org/10.1016/0012-821X(96)00121-5, 1996.

Heikkilä, U., Beer, J., and Feichter, J.: Meridional transport and deposition of atmospheric ^{10}Be, Atmospheric Chemistry and Physics, 9, 515–527, https://doi.org/10.5194/acp-9-515-2009, 2009.

Herrero-Bervera, E., Helsley, C. E., Sarna-Wojcicki, A. M., Lajoie, K. R., Meyer, C. E., McWilliams, M. O., Negrini, R. M., Turrin, B. D., Nolan, J. M. D., and Liddicoat, J. C.: Age and correlation of a paleomagnetic episode in the western United States by 40Ar/39Ar dating and tephrochronology: The Jamaica, Blake, or a new polarity episode?, Journal of Geophysical Research: Solid Earth, 99, 24091–24103, https://doi.org/10.1029/94JB01546, 1994.

Horiuchi, K., Uchida, T., Sakamoto, Y., Ohta, A., Matsuzaki, H., Shibata, Y., and Motoyama, H.: Ice core record of 10Be over the past millennium from Dome Fuji, Antarctica: A new proxy record of past solar activity and a powerful tool for stratigraphic dating, Quaternary Geochronology, 3, 253–261, https://doi.org/10.1016/j.quageo.2008.01.003, 2008.

Horiuchi, K., Kamata, K., Maejima, S., Sasaki, S., Sasaki, N., Yamazaki, T., Fujita, S., Motoyama, H., and Matsuzaki, H.: Multiple 10Be records revealing the history of cosmic-ray variations across the Iceland Basin excursion, Earth and Planetary Science Letters, 440, 105–114, https://doi.org/10.1016/j.epsl.2016.01.034, 2016.

Houghton, B. F., Wilson, C. J. N., McWilliams, M. O., Lanphere, M. A., Weaver, S. D., Briggs, R. M., and Pringle, M. S.: Chronology and dynamics of a large silicic magmatic system: Central Taupo Volcanic Zone, New Zealand, Geology, 23, 13–16, https://doi.org/10.1130/0091-7613(1995)023%253C0013:CADOAL%253E2.3.CO;2, 1995.

Jeromson, M. R., Fujioka, T., Fink, D., Simon, K., Post, A. L., Blaxell, M., Sánchez-Palacios, J. T., Enge, T. G., Beggs, C., and White, D. A.: Beryllium-isotope signatures in ice sheet proximal marine sediments, Chemical Geology, 691, 122912, https://doi.org/10.1016/j.chemgeo.2025.122912, 2025.

Johnson, M. O., Mudd, S. M., Pillans, B., Spooner, N. A., Keith Fifield, L., Kirkby, M. J., and Gloor, M.: Quantifying the rate and depth dependence of bioturbation based on optically-stimulated luminescence (OSL) dates and meteoric 10Be, Earth Surface Processes and Landforms, 39, 1188–1196, https://doi.org/10.1002/esp.3520, 2014.

Jouzel, J., Cauquoin, A., Bard, E., Zhang, L., Hou, S., Wu, Z., Zhou, W., Lipenkov, V., Petit, J.-R., Raisbeck, G., and Yiou, F.: Beryllium 10 in Antarctica over the last seven millennia, Sci Data, https://doi.org/10.1038/s41597-025-06444-0, 2026.

Kappelt, N., Muscheler, R., Baroni, M., Beer, J., Christl, M., Vockenhuber, C., Bard, E., and Wolff, E.: Ice core dating with the 36Cl/10Be ratio, Quaternary Science Reviews, 355, 109254, https://doi.org/10.1016/j.quascirev.2025.109254, 2025.

Kawamura, K., Parrenin, F., Lisiecki, L., Uemura, R., Vimeux, F., Severinghaus, J. P., Hutterli, M. A., Nakazawa, T., Aoki, S., Jouzel, J., Raymo, M. E., Matsumoto, K., Nakata, H., Motoyama, H., Fujita, S., Goto-Azuma, K., Fujii, Y., and Watanabe, O.: Northern Hemisphere forcing of climatic cycles in Antarctica over the past 360,000 years, Nature, 448, 912–916, https://doi.org/10.1038/nature06015, 2007.

Knudsen, M. F., Henderson, G. M., Frank, M., Mac Niocaill, C., and Kubik, P. W.: In-phase anomalies in Beryllium-10 production and palaeomagnetic field behaviour during the Iceland Basin geomagnetic excursion, Earth and Planetary Science Letters, 265, 588–599, https://doi.org/10.1016/j.epsl.2007.10.051, 2008.

Kok, Y. S. and Tauxe, L.: Saw-toothed pattern of sedimentary paleointensity records explained by cumulative viscous remanence, Earth and Planetary Science Letters, 144, E9–E14, https://doi.org/10.1016/S0012-821X(96)00175-6, 1996.

Korschinek, G., Bergmaier, A., Faestermann, T., Gerstmann, U. C., Knie, K., Rugel, G., Wallner, A., Dillmann, I., Dollinger, G., Von Gostomski, Ch. L., Kossert, K., Maiti, M., Poutivtsev, M., and Remmert, A.: A new value for the half-life of 10Be by Heavy-Ion Elastic Recoil Detection and liquid scintillation counting, Nuclear Instruments and Methods in Physics Research Section B: Beam Interactions with Materials and Atoms, 268, 187–191, https://doi.org/10.1016/j.nimb.2009.09.020, 2010.

Laj, C., Kissel, C., and Roberts, A. P.: Geomagnetic field behavior during the Iceland Basin and Laschamp geomagnetic excursions: A simple transitional field geometry?, Geochemistry, Geophysics, Geosystems, 7, https://doi.org/10.1029/2005GC001122, 2006.

Lal, D., Jull, A. J. T., Donahue, D. J., Burr, G. S., Deck, B., Jouzel, J., and Steig, E.: Record of cosmogenic in situ produced 14C in Vostok and Taylor Dome ice samples: Implications for strong role of wind ventilation processes, Journal of Geophysical Research: Atmospheres, 106, 31933–31941, https://doi.org/10.1029/2001JD900086, 2001.

Lamothe, A., Bard, E., THOUVENY, N., Ellyn, A., Severi, M., Traversi, R., de Angelis, M., Wilhelms, F., Mulvaney, R., Aster, T., and BARONI, M.: TALDICE 10Be and major ions 1470-1531 m, https://doi.org/10.5281/zenodo.17433639, 2025.

Lanci, L., Kissel, C., Leonhardt, R., and Laj, C.: Morphology of the Iceland Basin Excursion from a spherical harmonics analysis and an iterative Bayesian inversion procedure of sedimentary records, Physics of the Earth and Planetary Interiors, 169, 131–139, https://doi.org/10.1016/j.pepi.2008.06.004, 2008.

Langereis, C. G., Dekkers, M. J., de Lange, G. J., Paterne, M., and van Santvoort, P. J. M.: Magnetostratigraphy and astronomical calibration of the last 1.1 Myr from an eastern Mediterranean piston core and dating of short events in the Brunhes, Geophysical Journal International, 129, 75–94, https://doi.org/10.1111/j.1365-246X.1997.tb00938.x, 1997.

Leduc, G., Thouveny, N., Bourles, D., Blanchet, C., and Carcaillet, J.: Authigenic 10Be/9Be signature of the Laschamp excursion: A tool for global synchronisation of paleoclimatic archives, Earth and Planetary Science Letters, 245, 19–28, https://doi.org/10.1016/j.epsl.2006.03.006, 2006.

Legrand, M., Preunkert, S., Wolff, E., Weller, R., Jourdain, B., and Wagenbach, D.: Year-round records of bulk and size-segregated aerosol composition in central Antarctica (Concordia site) – Part 1: Fractionation of sea-salt particles, Atmospheric Chemistry and Physics, 17, 14039–14054, https://doi.org/10.5194/acp-17-14039-2017, 2017.

Lehman, B., Laj, C., Kissel, C., Mazaud, A., Paterne, M., and Labeyrie, L.: Relative changes of the geomagnetic field intensity during the last 280 kyear from piston cores in the A ores area, Physics of the Earth and Planetary Interiors, 1996.

Lisiecki, L. E. and Raymo, M. E.: A Pliocene-Pleistocene stack of 57 globally distributed benthic δ18O records, Paleoceanography, 20, https://doi.org/10.1029/2004PA001071, 2005.

Littot, G. C., Mulvaney, R., Röthlisberger, R., Udisti, R., Wolff, E. W., Castellano, E., Angelis, M. D., Hansson, M. E., Sommer, S., and Steffensen, J. P.: Comparison of analytical methods used for measuring major ions in the EPICA Dome C (Antarctica) ice core, Annals of Glaciology, 35, 299–305, https://doi.org/10.3189/172756402781817022, 2002.

Lund, S. P., Williams, T., Acton, G. D., Clement, B., and Okada, M.: 10. Brunhes Chron Magnetic Field Excursions Recovered from Leg 172 Sediments, 2001.

Mazaud, A.: 'Sawtooth' variation in magnetic intensity profiles and delayed acquisition of magnetization in deep sea cores, Earth and Planetary Science Letters, 139, 379–386, https://doi.org/10.1016/0012-821X(96)00026-X, 1996.

Mcwilliams, M.: Global Correlation of the 223 ka Pringle Falls Event, International Geology Review, 43, 191–195, https://doi.org/10.1080/00206810109465007, 2001.

Ménabréaz, L., Bourlès, D. L., and Thouveny, N.: Amplitude and timing of the Laschamp geomagnetic dipole low from the global atmospheric 10Be overproduction: Contribution of authigenic 10Be/9Be ratios in west equatorial Pacific sediments, Journal of Geophysical Research: Solid Earth, 117, https://doi.org/10.1029/2012JB009256, 2012.

Meynadier, L. and Valet, J.-P.: Post-depositional realignment of magnetic grains and asymmetrical saw-tooth patterns of magnetization intensity, Earth and Planetary Science Letters, 140, 123–132, https://doi.org/10.1016/0012-821X(96)00018-0, 1996.

Meynadier, L., Valet, J.-P., Guyodo, Y., and Richter, C.: Saw-toothed variations of relative paleointensity and cumulative viscous remanence: Testing the records and the model, Journal of Geophysical Research: Solid Earth, 103, 7095–7105, https://doi.org/10.1029/97JB03515, 1998.

Molina-Cardín, A., Dinis, L., and Osete, M. L.: Simple stochastic model for geomagnetic excursions and reversals reproduces the temporal asymmetry of the axial dipole moment, Proceedings of the National Academy of Sciences, 118, e2017696118, https://doi.org/10.1073/pnas.2017696118, 2021.

Morganti, A., Becagli, S., Castellano, E., Severi, M., Traversi, R., and Udisti, R.: An improved flow analysis–ion chromatography method for determination of cationic and anionic species at trace levels in Antarctic ice cores, Analytica Chimica Acta, 603, 190–198, https://doi.org/10.1016/j.aca.2007.09.050, 2007.

Müller, N. P., Gissinger, C., and Pétrélis, F.: Magnetic reversals in a geodynamo model with a stably-stratified layer, https://doi.org/10.48550/arXiv.2508.17777, 25 August 2025.

Muscheler, R., Beer, J., Kubik, P. W., and Synal, H.-A.: Geomagnetic field intensity during the last 60,000 years based on 10Be and 36Cl from the Summit ice cores and 14C, Quaternary Science Reviews, 24, 1849–1860, https://doi.org/10.1016/j.quascirev.2005.01.012, 2005.

Nowaczyk, N. R. and Frederichs, T. W.: Geomagnetic events and relative palaeointensity variations during the past 300 ka as recorded in Kolbeinsey Ridge sediments, Iceland Sea: indication for a strongly variable geomagnetic field, Int Journ Earth Sciences, 88, 116–131, https://doi.org/10.1007/s005310050250, 1999.

Oda, H., Nakamura, K., Ikehara, K., Nakano, T., Nishimura, M., and Khlystov, O.: Paleomagnetic record from Academician Ridge, Lake Baikal: a reversal excursion at the base of marine oxygen isotope stage 6, Earth and Planetary Science Letters, 202, 117–132, https://doi.org/10.1016/S0012-821X(02)00755-0, 2002.

ODP Leg 172 Scientific Party, Lund, S. P., Acton, G., Clement, B., Hastedt, M., Okada, M., and Williams, T.: Geomagnetic field excursions occurred often during the last million years, Eos, Transactions American Geophysical Union, 79, 178–179, https://doi.org/10.1029/98EO00134, 1998.

Oyabu, I., Kawamura, K., Buizert, C., Parrenin, F., Orsi, A., Kitamura, K., Aoki, S., and Nakazawa, T.: The Dome Fuji ice core DF2021 chronology (0–207 kyr BP), Quaternary Science Reviews, 294, 107754, https://doi.org/10.1016/j.quascirev.2022.107754, 2022.

Panovska, S., Poluianov, S., Gao, J., Korte, M., Mishev, A., Shprits, Y. Y., and Usoskin, I.: Effects of Global Geomagnetic Field Variations Over the Past 100,000 Years on Cosmogenic Radionuclide Production Rates in the Earth's Atmosphere, Journal of Geophysical Research: Space Physics, 128, e2022JA031158, https://doi.org/10.1029/2022JA031158, 2023.

Parrenin, F., Dreyfus, G., Durand, G., Fujita, S., Gagliardini, O., Gillet, F., Jouzel, J., Kawamura, K., Lhomme, N., Masson-Delmotte, V., Ritz, C., Schwander, J., Shoji, H., Uemura, R., Watanabe, O., and Yoshida, N.: 1-D-ice flow modelling at EPICA Dome C and Dome Fuji, East Antarctica, Climate of the Past, 3, 243–259, https://doi.org/10.5194/cp-3-243-2007, 2007.

Parrenin, F., Cavitte, M. G. P., Blankenship, D. D., Chappellaz, J., Fischer, H., Gagliardini, O., Masson-Delmotte, V., Passalacqua, O., Ritz, C., Roberts, J., Siegert, M. J., and Young, D. A.: Is there 1.5-million-year-old ice near Dome C, Antarctica?, The Cryosphere, 11, 2427–2437, https://doi.org/10.5194/tc-11-2427-2017, 2017.

Parrenin, F., Bouchet, M., Buizert, C., Capron, E., Corrick, E., Drysdale, R., Kawamura, K., Landais, A., Mulvaney, R., Oyabu, I., and Rasmussen, S. O.: The Paleochrono-1.1 probabilistic model to derive a common age model for several paleoclimatic sites using absolute and relative dating constraints, Geoscientific Model Development, 17, 8735–8750, https://doi.org/10.5194/gmd-17-8735-2024, 2024.

Pérez-Mejías, C., Moreno, A., Sancho, C., Bartolomé, M., Stoll, H., Cacho, I., Cheng, H., and Edwards, R. L.: Abrupt climate changes during Termination III in Southern Europe, Proceedings of the National Academy of Sciences, 114, 10047–10052, https://doi.org/10.1073/pnas.1619615114, 2017.

Poizat, M., Picard, G., Arnaud, L., Narteau, C., Amory, C., and Brun, F.: Widespread longitudinal snow dunes in Antarctica shaped by sintering, Nat. Geosci., 17, 889–895, https://doi.org/10.1038/s41561-024-01506-1, 2024.

Poluianov, S. V., Kovaltsov, G. A., Mishev, A. L., and Usoskin, I. G.: Production of cosmogenic isotopes 7Be, 10Be, 14C, 22Na, and 36Cl in the atmosphere: Altitudinal profiles of yield functions, Journal of Geophysical Research: Atmospheres, 121, 8125–8136, https://doi.org/10.1002/2016JD025034, 2016.

Railsback, L. B., Gibbard, P. L., Head, M. J., Voarintsoa, N. R. G., and Toucanne, S.: An optimized scheme of lettered marine isotope substages for the last 1.0 million years, and the climatostratigraphic nature of isotope stages and substages, Quaternary Science Reviews, 111, 94–106, https://doi.org/10.1016/j.quascirev.2015.01.012, 2015.

Raisbeck, G. M., Yiou, F., Bourles, D., and Kent, D. V.: Evidence for an increase in cosmogenic 10Be during a geomagnetic reversal, Nature, 315, 315–317, https://doi.org/10.1038/315315a0, 1985.

Raisbeck, G. M., Yiou, F., Cattani, O., and Jouzel, J.: 10Be evidence for the Matuyama–Brunhes geomagnetic reversal in the EPICA Dome C ice core, Nature, 444, 82–84, https://doi.org/10.1038/nature05266, 2006.

Raisbeck, G. M., Cauquoin, A., Jouzel, J., Landais, A., Petit, J.-R., Lipenkov, V. Y., Beer, J., Synal, H.-A., Oerter, H., Johnsen, S. J., Steffensen, J. P., Svensson, A., and Yiou, F.: An improved north–south synchronization of ice core records around the 41 kyr ^{10}Be peak, Climate of the Past, 13, 217–229, https://doi.org/10.5194/cp-13-217-2017, 2017.

Roberts, A. P., Lehman, B., Weeks, R. J., Verosub, K. L., and Laj, C.: Relative paleointensity of the geomagnetic field over the last 200,000 years from ODP Sites 883 and 884, North Pacific Ocean, Earth and Planetary Science Letters, 152, 11–23, https://doi.org/10.1016/S0012-821X(97)00132-5, 1997.

Ryan, D. A. and Sarson, G. R.: Are geomagnetic field reversals controlled by turbulence within the Earth's core?, Geophysical Research Letters, 34, https://doi.org/10.1029/2006GL028291, 2007.

Ryan, W. B. F.: Stratigraphy of late Quaternary sediments in the eastern Mediterranean, The Mediterranean Sea, 765, 1972.

Savranskaia, T., Egli, R., Valet, J.-P., Bassinot, F., Meynadier, L., Bourlès, D. L., Simon, Q., and Thouveny, N.: Disentangling magnetic and environmental signatures of sedimentary 10Be/9Be records, Quaternary Science Reviews, 257, 106809, https://doi.org/10.1016/j.quascirev.2021.106809, 2021.

Savranskaia, T., Egli, R., Simon, Q., Valet, J., Bassinot, F., and Thouveny, N.: Removing Climatic Overprints in Sedimentary Cosmogenic Beryllium Records: Potentials and Limits, Geochem Geophys Geosyst, 25, e2024GC011761, https://doi.org/10.1029/2024GC011761, 2024.

Severi, M., Becagli, S., Traversi, R., and Udisti, R.: Recovering Paleo-Records from Antarctic Ice-Cores by Coupling a Continuous Melting Device and Fast Ion Chromatography, Anal. Chem., 87, 11441–11447, https://doi.org/10.1021/acs.analchem.5b02961, 2015.

Shane, P., Black, T., and Westgate, J.: Isothermal plateau fission-Track age for a paleomagnetic excursion in the Mamaku Ignimbrite, New Zealand, and implications for Late Quaternary stratigraphy, Geophysical Research Letters, 21, 1695–1698, https://doi.org/10.1029/94GL01576, 1994.

Shibuya, H., Iwasaki, Y., Tanaka, H., and Hoshizumi, H.: Paleomagnetism of Unzen volcano: A volcanic record (Senbongi excursion) of the Iceland Basin event and the Brunhes VGP distribution for Japan, Earth Planet Sp, 59, 763–774, https://doi.org/10.1186/BF03352739, 2007.

Simon, Q., Thouveny, N., Bourlès, D. L., Valet, J.-P., Bassinot, F., Ménabréaz, L., Guillou, V., Choy, S., and Beaufort, L.: Authigenic 10Be/9Be ratio signatures of the cosmogenic nuclide production linked to geomagnetic dipole moment variation since the Brunhes/Matuyama boundary, Journal of Geophysical Research: Solid Earth, 121, 7716–7741, https://doi.org/10.1002/2016JB013335, 2016.

Simon, Q., Bourlès, D. L., Thouveny, N., Horng, C.-S., Valet, J.-P., Bassinot, F., and Choy, S.: Cosmogenic signature of geomagnetic reversals and excursions from the Réunion event to the Matuyama–Brunhes transition (0.7–2.14 Ma interval), Earth and Planetary Science Letters, 482, 510–524, https://doi.org/10.1016/j.epsl.2017.11.021, 2018.

Simon, Q., Thouveny, N., Bourlès, D. L., Valet, J.-P., and Bassinot, F.: Cosmogenic 10Be production records reveal dynamics of geomagnetic dipole moment (GDM) over the Laschamp excursion (20–60 ka), Earth and Planetary Science Letters, 550, 116547, https://doi.org/10.1016/j.epsl.2020.116547, 2020.

Singer, B. S., Jicha, B. R., Kirby, B. T., Geissman, J. W., and Herrero-Bervera, E.: 40Ar/39Ar dating links Albuquerque Volcanoes to the Pringle Falls excursion and the Geomagnetic Instability Time Scale, Earth and Planetary Science Letters, 267, 584–595, https://doi.org/10.1016/j.epsl.2007.12.009, 2008.

Stenni, B., Buiron, D., Frezzotti, M., Albani, S., Barbante, C., Bard, E., Barnola, J. M., Baroni, M., Baumgartner, M., Bonazza, M., Capron, E., Castellano, E., Chappellaz, J., Delmonte, B., Falourd, S., Genoni, L., Iacumin, P., Jouzel, J., Kipfstuhl, S., Landais, A., Lemieux-Dudon, B., Maggi, V., Masson-Delmotte, V., Mazzola, C., Minster, B., Montagnat, M., Mulvaney, R., Narcisi, B., Oerter, H., Parrenin, F., Petit, J. R., Ritz, C., Scarchilli, C., Schilt, A., Schüpbach, S., Schwander, J., Selmo, E., Severi, M., Stocker, T. F., and Udisti, R.: Expression of the bipolar see-saw in Antarctic climate records during the last deglaciation, Nature Geosci, 4, 46–49, https://doi.org/10.1038/ngeo1026, 2011.

Stoner, J. S., Channell, J. E. T., and Hillaire-Marcel, C.: A 200 ka geomagnetic chronostratigraphy for the Labrador Sea: Indirect correlation of the sediment record to SPECMAP, Earth and Planetary Science Letters, 159, 165–181, https://doi.org/10.1016/S0012-821X(98)00069-7, 1998.

Stoner, J. S., Channell, J. E. T., Hodell, D. A., and Charles, C. D.: A ∼580 kyr paleomagnetic record from the sub-Antarctic South Atlantic (Ocean Drilling Program Site 1089), Journal of Geophysical Research: Solid Earth, 108, https://doi.org/10.1029/2001JB001390, 2003.

Tachikawa, K., Timmermann, A., Vidal, L., Sonzogni, C., and Timm, O. E.: CO2 radiative forcing and Intertropical Convergence Zone influences on western Pacific warm pool climate over the past 400 ka, Quaternary Science Reviews, 86, 24–34, https://doi.org/10.1016/j.quascirev.2013.12.018, 2014.

Tanaka, H., Turner, G. M., Houghton, B. F., Tachibana, T., Kono, M., and McWilliams, M. O.: Palaeomagnetism and chronology of the central Taupo Volcanic Zone, New Zealand, Geophysical Journal International, 124, 919–934, https://doi.org/10.1111/j.1365-246X.1996.tb05645.x, 1996.

Tauxe, L. and Wu, G.: Normalized remanence in sediments of the western equatorial Pacific: Relative paleointensity of the geomagnetic field?, Journal of Geophysical Research: Solid Earth, 95, 12337–12350, https://doi.org/10.1029/JB095iB08p12337, 1990.

Thouveny, N., Carcaillet, J., Moreno, E., Leduc, G., and Nérini, D.: Geomagnetic moment variation and paleomagnetic excursions since 400 kyr BP: a stacked record from sedimentary sequences of the Portuguese margin, Earth and Planetary Science Letters, 219, 377–396, https://doi.org/10.1016/S0012-821X(03)00701-5, 2004.

Traversi, R., Becagli, S., Castellano, E., Marino, F., Rugi, F., Severi, M., Angelis, M. de, Fischer, H., Hansson, M., Stauffer, B., Steffensen, J. P., Bigler, M., and Udisti, R.: Sulfate Spikes in the Deep Layers of EPICA-Dome C Ice Core: Evidence of Glaciological Artifacts, Environ. Sci. Technol., 43, 8737–8743, https://doi.org/10.1021/es901426y, 2009.

Valet, J. and Meynadier, L.: Geomagnetic field intensity and reversals during the past four million years, Nature, 366, 234–238, https://doi.org/10.1038/366234a0, 1993.

Valet, J.-P., Meynadier, L., and Guyodo, Y.: Geomagnetic dipole strength and reversal rate over the past two million years, Nature, 435, 802–805, https://doi.org/10.1038/nature03674, 2005.

Valet, J.-P., Plenier, G., and Herrero-Bervera, E.: Geomagnetic excursions reflect an aborted polarity state, Earth and Planetary Science Letters, 2008.

Valet, J.-P., Thevarasan, A., Bassinot, F., Savranskaia, T., and Haddam, N.: Two Records of Relative Paleointensity for the Past 4 Myr, Front. Earth Sci., 8, https://doi.org/10.3389/feart.2020.00148, 2020.

Valet, J.-P., Savranskaia, T., Egli, R., Simon, Q., Bassinot, F., and Thouveny, N.: Beryllium ten production and relative paleointensity for the past 1.2 million years, Quaternary Science Reviews, 344, 108993, https://doi.org/10.1016/j.quascirev.2024.108993, 2024.

Valet, J.-P., Savranskaia, T., Simon, Q., Egli, R., Bassinot, F., and Thouveny, N.: Geomagnetic moment variation over the last 4.4 Million years through high resolution paleointensity and 10Be production records along ocean sediment sequences, Quaternary Science Reviews, 359, 109367, https://doi.org/10.1016/j.quascirev.2025.109367, 2025.

Weeks, R. J., Laj, C., Endignoux, L., Mazaud, A., Labeyrie, L., Roberts, A. P., Kissel, C., and Blanchard, E.: Normalised natural remanent magnetisation intensity during the last 240 000 years in piston cores from the central North Atlantic Ocean: geomagnetic field intensity or environmental signal?, Physics of the Earth and Planetary Interiors, 87, 213–229, https://doi.org/10.1016/0031-9201(94)02966-F, 1995.

Wille, J. D., Favier, V., Gorodetskaya, I. V., Agosta, C., Kittel, C., Beeman, J. C., Jourdain, N. C., Lenaerts, J. T. M., and Codron, F.: Antarctic Atmospheric River Climatology and Precipitation Impacts, Journal of Geophysical Research: Atmospheres, 126, e2020JD033788, https://doi.org/10.1029/2020JD033788, 2021.

Wolff, E. W., Fischer, H., van Ommen, T., and Hodell, D. A.: Stratigraphic templates for ice core records of the past 1.5 Myr, Climate of the Past, 18, 1563–1577, https://doi.org/10.5194/cp-18-1563-2022, 2022.

Yamamoto, Y., Shibuya, H., Tanaka, H., and Hoshizumi, H.: Geomagnetic paleointensity deduced for the last 300 kyr from Unzen Volcano, Japan, and the dipolar nature of the Iceland Basin excursion, Earth and Planetary Science Letters, 293, 236–249, https://doi.org/10.1016/j.epsl.2010.02.024, 2010.

Yamazaki, T. and Ioka, N.: Long-term secular variation of the geomagnetic field during the last 200 kyr recorded in sediment cores from the western equatorial Pacific, Earth and Planetary Science Letters, 128, 527–544, https://doi.org/10.1016/0012-821X(94)90168-6, 1994.

Yamazaki, T., Ioka, N., and Eguchi, N.: Relative paleointensity of the geomagnetic field during the Brunhes Chron, Earth and Planetary Science Letters, 136, 525–540, https://doi.org/10.1016/0012-821X(95)00189-J, 1995.

Yiou, F., Raisbeck, G. M., Bourles, D., Lorius, C., and Barkov, N. I.: 10Be in ice at Vostok Antarctica during the last climatic cycle, Nature, 316, 616–617, https://doi.org/10.1038/316616a0, 1985.

Zheng, M., Adolphi, F., Ferrachat, S., Mekhaldi, F., Lu, Z., Nilsson, A., and Lohmann, U.: Modeling Atmospheric Transport of Cosmogenic Radionuclide 10Be Using GEOS-Chem 14.1.1 and ECHAM6.3-HAM2.3: Implications for Solar and Geomagnetic Reconstructions, Geophysical Research Letters, 51, e2023GL106642, https://doi.org/10.1029/2023GL106642, 2024.